Dimethylsulfide (DMS) production in polar oceans may be resilient to ocean acidification.

Frances E. Hopkins[1], Philip D. Nightingale[1], John A. Stephens[1], C. Mark Moore[2], Sophie Richier[2], Gemma L. Cripps[2], Stephen D. Archer[3]

5   [1]Plymouth Marine Laboratory, Plymouth, PL1 3DH, U.K.

[2]Ocean and Earth Science, National Oceanography Centre, University of Southampton, Southampton, U.K.

[3]Bigelow Laboratory for Ocean Sciences, Maine, U.S.A.

Correspondence to: Frances E. Hopkins (fhop@pml.ac.uk)

10   **Abstract.** Emissions of dimethylsulfide (DMS) from the polar oceans play a key role in
atmospheric processes and climate. Therefore, it is important we increase our understanding
of how DMS production in these regions may respond to environmental change. The polar
oceans are particularly vulnerable to ocean acidification (OA). However, our understanding
of the polar DMS response is limited to two studies conducted in Arctic waters, where in both

15   cases DMS concentrations decreased with increasing acidity. Here, we report on our findings
from seven summertime shipboard microcosm experiments undertaken in a variety of
locations in the Arctic Ocean and Southern Ocean. These experiments reveal no significant
effects of short term OA on the net production of DMS by planktonic communities. This is in
contrast to identical experiments from temperate NW European shelf waters where surface

20   ocean communities responded to OA with significant increases in dissolved DMS
concentrations. A meta-analysis of the findings from both temperate and polar waters ($n = 18$
experiments) reveals clear regional differences in the DMS response to OA. We suggest that
these regional differences in DMS response reflect the natural variability in carbonate
chemistry to which the respective communities may already be adapted. Future temperate

25   oceans could be more sensitive to OA resulting in a change in DMS emissions to the
atmosphere, whilst perhaps surprisingly DMS emissions from the polar oceans may remain

relatively unchanged. By demonstrating that DMS emissions from geographically distinct

regions may vary in response to OA, our results may facilitate a better understanding of

Earth's future climate. Our study suggests that the way in which processes that generate DMS

30   respond to OA may be regionally distinct and this should be taken into account in predicting

future DMS emissions and their influence on Earth's climate.

1 Introduction

The trace gas dimethylsulfide (DMS) is a key ingredient in a cocktail of gases that exchange

between the ocean and atmosphere. Dissolved DMS is produced via the enzymatic

35   breakdown of dimethylsulfoniopropionate (DMSP), a secondary algal metabolite implicated

in a number of cellular roles, including the regulation of carbon and sulfur metabolism via an

overflow mechanism (Stefels 2000) and protection against oxidative stress (Sunda et al.

2002). Oceanic DMS emissions amount to 17 - 34 Tg S y^{-1}, representing 80 - 90% of all

marine biogenic S emissions, and up to 50% of global biogenic emissions (Lana et al. 2011).

40   DMS and its oxidation products play vital roles in atmospheric chemistry and climate

processes. These processes include aerosol formation pathways that influence the

concentration of cloud condensation nuclei (CCN) with implications for Earth's albedo and

climate (Charlson et al. 1987; Korhonen et al. 2008), and the atmospheric oxidation pathways

of other key climate gases, including isoprene, ammonia and organohalogens (von Glasow

45   and Crutzen 2004; Johnson and Bell 2008; Chen and Jang 2012). Thus, our ability to predict

the climate into the future requires an understanding of how marine DMS production may

respond to global change (Carpenter et al. 2012; Woodhouse et al. 2013).

The biologically-rich seas surrounding the Arctic pack ice are a strong source of DMS to the

Arctic atmosphere (Levasseur 2013). A seasonal cycle in CCN numbers can be related to

50   seasonality in the Arctic DMS flux (Chang et al. 2011). Indeed, observations confirm that

DMS oxidation products promote the growth of particles to produce aerosols that may
influence cloud processes and atmospheric albedo (Bigg and Leck 2001; Korhonen et al.
2008; Chang et al. 2011; Rempillo et al. 2011). Arctic new particle formation events and
peaks in aerosol optical depth (AOD) occur during summertime clean air periods (when

55   levels of anthropogenic black carbon diminish), and have been linked to chlorophyll *a*
maxima and the presence of biogenic aerosols formed from DMS oxidation such as
methanesulfonate (MSA). The atmospheric oxidation products of DMS - SO_2 and H_2SO_4 -
contribute to both the growth of existing particles and new particle formation (NPF) in the
Arctic atmosphere (Sharma et al. 2012; Leaitch et al. 2013; Gabric et al. 2014). Thus, the

60   ongoing and projected rapid loss of seasonal Arctic sea ice may influence the Arctic radiation
budget via changes to both the DMS flux and the associated formation and growth of cloud-
influencing particles (Sharma et al. 2012).

During its short but highly productive summer season, the Southern Ocean is a hotspot of
DMS flux to the atmosphere, influenced by the prevalence of intense blooms of DMSP-rich

65   *Phaeocystis antarctica* (Schoemann et al. 2005) and the presence of persistent high winds
particularly in regions north of the sub-Antarctic front (Jarníková and Tortell 2016). Around
3.4 Tg of sulfur is released to the atmosphere between December and February, a flux that
represents ~15 % of global annual emissions of DMS (Jarníková and Tortell 2016). Elevated
CCN numbers are seen in the most biologically active regions of the Southern Ocean, with a

70   significant contribution from DMS-driven secondary aerosol formation processes (Korhonen
et al. 2008; McCoy et al. 2015). DMS-derived aerosols from this region are estimated to
contribute 6 to 10 W m^{-2} to reflected short wavelength radiation, similar to the influence of
anthropogenic aerosols in the polluted Northern Hemisphere (McCoy et al. 2015). Given this
important influence of polar DMS emissions on atmospheric processes and climate, it is vital

75 we increase our understanding of the influence of future ocean acidification on DMS

production.

The polar oceans are characterised by high dissolved inorganic carbon (DIC) concentrations

and a low carbonate system buffering capacity, mainly due to the increased solubility of CO_2

in cold waters (Sabine et al. 2004; Orr et al. 2005). This makes these regions particularly

80 susceptible to the impacts of ocean acidification (OA). For example, extensive carbonate

mineral undersaturation is expected to occur in Arctic waters within the next 20 – 80 years

(McNeil and Matear 2008; Steinacher et al. 2009). OA has already led to a 0.1 unit decrease

in global surface ocean pH, with a further fall of ~0.4 units expected by the end of the century

(Orr et al. 2005). The greatest declines in pH are likely in the Arctic Ocean with a predicted

85 fall of 0.45 units by 2100 (Steinacher et al. 2009). The potential effects of OA on marine

organisms, communities and ecosystems could be wide-ranging and severe, due in part to the

speed and extent of a change not seen on Earth for at least 300 Ma (Raven et al. 2005;

Hönisch et al. 2012). Despite the imminent threat to polar ecosystems and the importance of

DMS emissions to atmospheric processes, our knowledge of the response of polar DMS

90 production to OA is limited to a single mesocosm experiment performed in a coastal fjord in

Svalbard (Archer et al. 2013; Riebesell et al. 2013) and one shipboard microcosm experiment

with seawater collected from Baffin Bay (Hussherr et al. 2017). Both studies reported

significant reductions in DMS concentrations with increasing levels of pCO$_2$ during seasonal

phytoplankton blooms. However, these two studies may not be fully representative of the

95 response of the open Arctic or Southern Oceans due to their coastal locations.

Mesocosm experiments are a critical tool for assessing OA effects on surface ocean

communities. Initial studies focused on the growth and decline of blooms with (Engel et al.

2005; Kim et al. 2006; Engel et al. 2008; Schulz et al. 2008; Hopkins et al. 2010; Kim et al.

2010; Schulz et al. 2013; Webb et al. 2015), or without (Crawfurd et al. 2016; Webb et al.

100   2016) the addition of inorganic nutrients. The response of DMS to OA has been examined

several times, predominantly at the same site in Norwegian coastal waters (Vogt et al. 2008;

Hopkins et al. 2010; Avgoustidi et al. 2012; Webb et al. 2015). There have also been two

studies in Korean coastal waters (Kim et al. 2010; Park et al. 2014), as well as the single

mesocosm study in the coastal (sub) Arctic waters of Svalbard (Archer et al. 2013).

105   Mesocosm enclosures, ranging in volume from ~11,000 – 50,000 L, allow the response of

surface ocean communities to a range of CO_2 treatments to be monitored under near-natural

light and temperature conditions over time scales (weeks - months) that allow a 'winners vs

loser' dynamic to develop. The response of DMS cycling to elevated CO_2 is generally driven

by changes to the microbial community structure (Engel et al. 2008; Hopkins et al. 2010;

110   Archer et al. 2013; Brussaard et al. 2013). The size and construction of the mesocosms has

limited their deployment to coastal/sheltered waters, resulting in minimal geographical

coverage, and leaving large gaps in our understanding of the response of open ocean

phytoplankton communities to OA.

Here, we adopt an alternative but complementary approach to explore the effects of OA on

115   the cycling of DMS with the use of short-term shipboard microcosm experiments. We build

on the previous temperate NW European shelf studies of Hopkins & Archer (2014) by

extending our experimental approach to the Arctic and Southern Oceans. Vessel-based

research enables multiple short term (days) identical incubations to be performed over

extensive spatial scales, that encompass natural gradients in carbonate chemistry, temperature

120   and nutrients (Richier et al. 2014; Richier et al. under review). This allows an assessment to

be made of how a range of surface ocean communities, adapted to a variety of environmental

conditions, respond to the same driver. The focus is then on the effect of short-term CO_2

exposure on physiological processes, as well as the extent of the variability in adaptive

capacity between communities. The level of adaptive capacity within an ecosystem

125 determines the level of resilience to changing environmental conditions. Therefore, do

spatially-diverse communities respond differently to short term OA, and can this be explained

by the range of environmental conditions to which each is presumably already adapted? The

rapid CO_2 changes implemented in this study, and during mesocosm studies, are far from

representative of the predicted rate of change to seawater chemistry over the coming decades.

130 Nevertheless, our approach can provide insight into the physiological response of a variety of

polar surface ocean communities, as well as their potential adaptive capacity to future OA

when compared between environments that differ in carbonate chemistry (Stillman and

Paganini 2015), alongside the implications this may have for DMS production.

Communities of the NW European shelf consistently responded to acute OA with significant

135 increases in net DMS production, likely a result of an increase in stress-induced algal

processes (Hopkins and Archer 2014). Do polar phytoplankton communities, which are

potentially adapted to contrasting biogeochemical environments, respond in the same way?

By expanding our approach to encompass both polar oceans, we can assess regional contrasts

in response. To this end, we combine our findings for temperate waters with those for the

140 polar oceans into a meta-analysis to advance our understanding of the regional variability and

drivers in the DMS response to OA.

2 Material and Methods

2.1 Sampling stations

This study presents new data from two sets of field experiments carried out as a part of the

145 UK Ocean Acidification Research Programme (UKOA) aboard the RRS James Clark Ross in

the sub-Arctic and Arctic in June-July 2012 (JR271) and in the Southern Ocean in January-

February 2013 (JR274). Data are combined with the results from an earlier study on board the

RRS Discovery (D366) described in Hopkins & Archer (2014). In total, 18 incubations were

performed; 11 in temperate and sub-Arctic waters of the NW European shelf and North

150   Atlantic, 3 in Arctic waters and 4 in the Southern Ocean. Figure 1 shows the cruise tracks,

surface concentrations of DMS and total DMSP (DMSPt) at CTD sampling stations as well

as the locations of sampling for shipboard microcosms (See Table 1 for further details).

2.2 Shipboard microcosm experiments

The general design and implementation of the experimental microcosms for JR271 and

155   JR274 was essentially the same as for D366 and described in Richier et al. (2014) and

Hopkins & Archer (2014), but with the additional adoption of trace metal clean sampling and

incubation techniques in the low trace metal open ocean waters (see Richier et al. (under

review)). At each station water was collected pre-dawn within the mixed layer from three

successive separate casts of a trace-metal clean titanium CTD rosette comprising twenty-four

160   10 L Niskin bottles. Each cast was used to fill one of a triplicated set of experimental bottles

(locations and sample depths, Table 1). Bottles were sampled within a class-100 filtered air

environment within a trace metal clean container to avoid contamination during the set up.

The water was directly transferred into acid-cleaned 4.5 L polycarbonate bottles using acid-

cleaned silicon tubing, with no screening or filtration.

165   The carbonate chemistry within the experimental bottles was manipulated by addition of

equimolar HCl and $NaHCO_3^-$ (1 mol L^{-1}) to achieve a range of target CO_2 values (550, 750,

1000, 2000 µatm) (Gattuso et al. 2010). For the sub-Arctic/Arctic microcosms, additions

were used to attain three target CO_2 levels (550 µatm, 750 µatm and 1000 µatm). For

Southern Ocean experiments, two experiments (*Drake Passage* and *Weddell Sea*) underwent

170   combined CO_2 and Fe additions (ambient, Fe (2 nM), high CO_2 (750 µatm), Fe (2 nM) + high

CO_2 (750µatm) (only high CO_2 treatments will be examined here; no response to Fe was

detected in DMS or DMSP concentrations). Three CO_2 treatments (750 µatm, 1000 µatm,

2000 µatm) were tested in the last two experiments (*South Georgia* and *South Sandwich*).

After first ensuring the absence of bubbles or headspace, the bottles were sealed with high

175   density polyethylene (HDPE) lids with silicone/ polytetrafluoroethylene (PTFE) septa and

placed in the incubation container. Bottles were incubated inside a custom-designed

temperature- and light-controlled shipping container, set to match the *in situ* water

temperature at the time of water collection. A constant light level ($100 \ \mu E \ m^{-2} \ s^{-1}$) was

provided by daylight simulating LED panels (Powerpax, UK). The light period within the

180   microcosms was representative of *in situ* conditions. For the sub-Arctic/Arctic Ocean

stations, experimental bottles were subjected to continuous light representative of the 24 h

daylight of the Arctic summer. For Southern Ocean stations, an 18:6 light: dark cycle was

used. Each bottle belonged to a set of triplicates, and sacrificial sampling of bottles was

performed (see Table 1 for chosen time points). Use of three sets of triplicates for each time

185   point allowed for the sample requirements of the entire scientific party (3 x 3 bottles, x 2 time

points (T_1, T_2), x 4 CO_2 treatments = 72 bottles in total). Incubation times were extended for

Southern Ocean stations *Weddell Sea*, *South Georgia* and *South Sandwich* (see Table 1) as

minimal CO_2 response, attributed to slower microbial metabolism at low water temperatures,

was observed for the first Southern Ocean station *Drake Passage* over 96 h (see also Richier

190   et al. (under review)). Samples for carbonate chemistry measurements were made first,

followed by sampling for DMS, DMSP and related parameters.

2.3 Standing stocks of DMS and DMSP

Methods for the determination of seawater concentrations of DMS and DMSP are identical to

those described in Hopkins & Archer (2014) and will therefore be described in brief here.

195   Seawater DMS concentrations were determined by cryogenic purge and trap, with gas

chromatography and pulsed flame photometric detection (Archer et al., 2013). Samples for

total DMSP concentrations were fixed by addition of 35 µl of 50 % H_2SO_4 to 7 mL of

seawater (Kiene and Slezak 2006), and analysed within 2 months of collection (Archer et al.

2013). Concentrations of DMSPp were determined at each time point by gravity filtering 7

200   ml of sample onto a 25 mm GF/F filter and preserving the filter in 7 ml of 35 mM H_2SO_4 in

MQ-water. DMSP concentrations were subsequently measured as DMS following alkaline

hydrolysis. DMS calibrations were performed using alkaline cold-hydrolysis (1 M NaOH) of

DMSP sequentially diluted three times in MilliQ water to give working standards in the range

0.03 – 3.3 ng S mL^{-1}. Five point calibrations were performed every 2 – 4 days throughout the

205   cruise.

2.4 *De novo* DMSP synthesis

De novo DMSP synthesis and gross production rates were determined for all microcosm

experiments at each experimental time point, using methods based on the approach of Stefels

et al. (2009) and described in detail in Archer et al. (2013) and Hopkins and Archer (2014).

210   Triplicate rate measurements were determined for each CO_2 level. For each rate measurement

three x 500 mL polycarbonate bottles were filled by gently siphoning water from each

replicate microcosm bottle. Trace amounts of $NaH^{13}CO_3$, equivalent to ~6 % of *in situ*

dissolved inorganic carbon (DIC), were added to each 500 mL bottle. The bottles were

incubated in the microcosm incubation container with temperature and light levels as

215   described earlier. Samples were taken at 0 h, then at two further time points over a 6 - 9 h

period. At each time point, 250 mL was gravity filtered in the dark through a 47 mm GF/F

filter, the filter gently folded and placed in a 20 mL serum vial with 10 mL of Milli-Q and

one NaOH pellet, and the vial was crimp-sealed. Samples were stored at -20°C until analysis

by proton transfer reaction-mass spectrometer (PTR-MS) (Stefels et al. 2009).

220   The specific growth rate of DMSP (µDMSP) was calculated assuming exponential growth

from:

$$\mu_t(\Delta t^{-1}) = \alpha_k \times AVG\left[\ln\left(\frac{^{64}MP_{eq} - {}^{64}MP_{t-1}}{^{64}MP_{eq} - {}^{64}MP_{t}}\right), \ln\left(\frac{^{64}MP_{eq} - {}^{64}MP_{t}}{^{64}MP_{eq} - {}^{64}MP_{t+1}}\right)\right]$$

(Stefels et al. 2009) where $^{64}MP_t$, $^{64}MP_{t-1}$, $^{64}MP_{t+1}$ are the proportion of 1 x ^{13}C labelled

DMSP relative to total DMSP at time t, at the preceding time point (t-1) and at the subsequent

225   time point (t+1), respectively. Values of ^{64}MP were calculated from the protonated masses of

DMS as: mass 64/(mass63+mass64+mass65), determined by PTR-MS. $^{64}MP_{eq}$ is the

theoretical equilibrium proportion of 1 x ^{13}C based on a binomial distribution and the

proportion of tracer addition. An isotope fractionation factor α_k of 1.06 is included, based on

laboratory culture experiments using *Emiliania huxleyi* (Stefels et al. 2009). Gross DMSP

230   production rates during the incubations (nmol L^{-1} h^{-1}) were calculated from μDMSP and the

initial particulate DMSP (DMSPp) concentration of the incubations (shown in Figure 4).

2.5 Seawater carbonate chemistry analysis

The techniques and methods used to determine both the *in situ* and experimental carbonate

chemistry parameters, and to manipulate seawater carbonate chemistry within the

235   microcosms, are described in Richier et al. (2014) and will be only given in brief here.

Experimental T_0 measurements were taken directly from CTD bottles, and immediately

measured for total alkalinity (T_A) (Apollo SciTech Ct analyser (AS-C3) with LI-COR 7000)

and dissolved inorganic carbon (DIC) (Apollo SciTech AS-Alk2 Alkalinity Titrator). The

CO2SYS programme (version 1.05) (Lewis and Wallace 1998) was used to calculate the

240   remaining carbonate chemistry parameters including pCO$_2$.

Measurements of T_A and DIC were made from each bottle at each experimental time point

and again used to calculate the corresponding values for pCO$_2$ and pH$_T$. The data at T_1 and T_2

of each experiment and each CO_2 treatment level are summarised in Supplementary Table S1

and Supplementary Table S2 (T_0 data are given in Table 1).

245   **2.6 Chlorophyll a (Chl *a*) determinations**

Concentrations of Chl *a* were determined as described in Richier et al. (2014). Briefly, 100

mL aliquots of seawater from the incubation bottles were filtered through either 25 mm GF/F

(Whatman, 0.7 μm pore size) or polycarbonate filters (Whatman, 10 μm pore size) to yield

total and >10 μm size fractions, with the <10 μm fraction calculated by difference. Filters

250   were extracted in 6 mL HPLC-grade acetone (90%) overnight in a dark refrigerator.

Fluorescence was measured using a Turner Designs Trilogy fluorometer, which was regularly

calibrated with dilutions of pure Chl *a* (Sigma, UK) in acetone (90%).

2.7 Relative growth rate (RGR)

Relative growth rate (RGR), an indicator of the level of net autotrophy within the

255   experimental microcosms, was calculated as the change in Chl *a* concentrations between the

first two experimental time points:

$$RGR = \frac{(ln(C1)) - (ln(C0))}{T1 - T0}$$ 2

Where C_0 and C_1 are Chl *a* concentration at experimental time points T_0 and T_1, and T is time

in days.

260   **2.8 Data handling and statistical analyses**

Permutational analysis of variance (PERMANOVA) was used to analyse the difference in

response of DMS and DMSP concentrations to OA, both between and within the two polar

cruises in this study. Both dependant variables were analysed separately using a nested

factorial design with three factors; (i) Cruise Location: Arctic and Southern Ocean, (ii)

265   Experiment location nested within Cruise location: E1- E4/E5, and (iii) CO_2 level: 385, 550,

750, 1000 and 2000 µatm. Main effects and pairwise comparisons of the different factors

were analysed through unrestricted permutations of raw data. If a low number of

permutations were generated then the *p*-value was obtained through random sampling of the

asymptotic permutation distribution, using Monte Carlo tests.

270   One-way analysis of variance was used to identify differences in ratio of >10 µm Chl *a* to

total Chl *a* ($chl_{>10um}$: chl_{tot} , see Discussion). Initially, tests of normality were applied ($p<0.05$

= not normal), and if data failed to fit the assumptions of the test, linearity transformations of

the data were performed (logarithmic or square root), and the ANOVA proceeded from this

point. The results of ANOVA are given as follows: *F* = ratio of mean squares, *df* = degrees of

275   freedom, *p* = level of confidence. For those data still failing to display normality following

transformation, a rank-based Kruskal-Wallis test was applied (*H* = test statistic, *df* = degrees

of freedom, *p* = level of confidence).

3 Results

3.1 Sampling stations

280   Seawater temperatures at the microcosm sampling stations ranged from -1.5°C at sea-ice

influenced stations (*Greenland Ice-edge* and *Weddell Sea*) up to 6.5°C for *Barents Sea* (Fig. 2

A). Salinity values at all the Southern Ocean stations were <34, whilst they were ~35 at all

the Arctic stations with the exception of *Greenland Ice-edge* which had the lowest salinity of

32.5 (Fig. 2 B). Phototrophic nanoflagellate abundances were variable, with >3 x 10^4 cells

285   mL^{-1} at *Greenland Gyre*, 1.5 x 10^4 cells mL^{-1} at *Barents Sea* and <3 x 10^3 cells mL^{-1} for all

other stations (Fig. 2 D). Total bacterial abundances ranged from 3 x 10^5 cells mL^{-1} at

Greenland Ice-edge up to 3 x 10^6 cells mL^{-1} at *Barents Sea* (Fig. 2 E). Chl *a* concentrations

were similarly variable, exceeding 4 µg L^{-1} at *South Sandwich* and 2 µg L^{-1} at *Greenland Ice-*

edge, whilst the remaining stations ranged from 0.2 µg L^{-1} (*Weddell Sea*) to 1.5 µg L^{-1} (Fig. 2

290 F).

The high Chl *a* concentrations at *South Sandwich* are reflected in low in-water irradiance

levels at this station (Fig. 2 C). Surface DMS concentrations ranged from 1 – 3 nmol L^{-1}, with

the exception of *South Sandwich* where concentrations of ~12 nmol L^{-1} were observed (Fig. 2

G). DMSP generally ranged from 12 – 20 nmol L^{-1}, except *Barents Sea* where surface

295 concentrations exceeded 60 nmol L^{-1} (Fig. 2 H).

3.2 Response of DMS and DMSP to OA

The temporal trend in DMS concentrations showed a similar pattern for the three Arctic

Ocean experiments. Initial concentrations of 1 – 2 nmol L^{-1} remained relatively constant over

the first 48 h and then showed small increases of 1 - 4 nmol L^{-1} over the incubation period

300 (Figure 3 A – C). No significant effects of elevated CO_2 on DMS concentrations were

observed. Initial DMSP concentrations were more variable, from 6 nmol L^{-1} at *Greenland

Ice-edge* to 12 nmol L^{-1} at *Barents Sea*, and either decreased slightly (net loss 1 – 2 nmol L^{-1}

GG), or increased slightly (net increase ~4 nmol L^{-1} *Greenland Ice-edge*, ~3 nmol L^{-1} *Barents

Sea*) (Figure 4 A – C). DMSP concentrations were found to increase significantly in response

305 to elevated CO_2 after 48 h for *Barents Sea* (Fig. 4 C, $t = 2.05$, $p = 0.025$), but no other

significant responses in DMSP were identified.

The range of initial DMS concentrations was greater at Southern Ocean sampling stations

compared to the Arctic, from 1 nmol L^{-1} at *Drake Passage* up to 13 nmol L^{-1} at *South

Sandwich* (Figure 3 D – G). DMS concentrations showed little change over the course of 96 –

310 168 h incubations and no effect of elevated CO_2, with the exception of *South Sandwich* (Fig.

3 G). Here, concentrations decreased sharply after 96 h by between 3 and 11 nmol L^{-1}.

Concentrations at 96 h were CO_2-treatment dependent, with significant decreases in DMS

concentration occurring with increasing levels of CO_2 (PERMANOVA, $t = 2.61$, $p = 0.028$).

Significant differences ceased to be detectable by the end of the incubations (168 h).

315   Initial DMSP concentrations were higher than for Arctic stations, ranging from 13 nmol L^{-1}

for *Weddell Sea* to 40 nmol L^{-1} for *South Sandwich* (Figure 4 D – G). Net increases in DMSP

occurred throughout, and were on the order of between <10 nmol L^{-1} - >30 nmol L^{-1} over the

course of the incubations. Concentrations were not generally $p CO_2$-treatment dependent with

the exception of the final time point at *South Georgia* (144 h) when a significant decrease in

320   DMSP with increasing CO_2 was observed (PERMANOVA, $t = -5.685$, $p<0.001$).

3.3 Response of de novo DMSP synthesis and production to OA

Rates of *de novo* DMSP synthesis (μDMSP) at initial time points (T_0) ranged from 0.13 d^{-1}

(*Weddell Sea*, Fig. 5 G) to 0.23 d^{-1} (*Greenland Ice-edge*, Fig. 5 C), whilst DMSP production

ranged from 0.4 nmol L^{-1} d^{-1} (*Greenland Gyre*, Fig. 5 B) to 2.27 nmol L^{-1} d^{-1} (*Drake Passage*,

325   Fig. 5 F). Maximum rates of μDMSP of 0.37 -0.38 d^{-1} were observed at *Greenland Ice-edge*

after 48 h of incubation in all CO_2 treatments (Fig. 5 C). The highest rates of DMSP

production were observed at *South Georgia* after 96 h of incubation, and ranged from 4.1 –

6.9 nmol L^{-1} d^{-1} across CO_2 treatments (Fig. 5 J). Rates of DMSP synthesis and production

were generally lower than those measured in temperate waters (Hopkins and Archer 2014)

330   (Initial rates: μDMSP 0.33 – 0.96 d^{-1}, 7.1 – 37.3 nmol L^{-1} d^{-1}), but were comparable to

measurements made during an Arctic mesocosm experiment (Archer et al. 2013) (0.1 – 0.25

d^{-1}, 3 – 5 nmol L^{-1} d^{-1} in non-bloom conditions). The lower rates in cold polar waters likely

reflect slower metabolic processes and are reflected by standing stock DMSP concentrations

which were also lower than in temperate waters (5 – 40 nmol L^{-1} polar, 8 – 60 nmol L^{-1}

335   temperate (Hopkins and Archer 2014)). No consistent evidence of CO_2 sensitivity was seen in

either DMSP synthesis or production, similar to findings for DMSP standing stocks. Some

notable but conflicting differences between CO_2 treatments were observed. There was a 36% and 37% increase in µDMSP and DMSP production respectively at 750 µatm for the *Drake Passage* after 96 h (Figure 5 E, F), and a 38% and 44% decrease in both at 750 µatm after

340   144 h for *Weddell Sea* (Figure 5 G, H). Nevertheless, no consistent and significant effects of high CO_2 were observed for rates of *de novo* DMSP synthesis or DMSP production in polar waters.

4 Discussion

4.1 Regional differences in the response of DMS(P) to OA

345   We combine our findings from the polar oceans with those from temperate waters into a meta-analysis in order to assess the regional variability and drivers in the DMS(P) response to OA. Figures 6 and 7 provide an overview of the results discussed so far in this current study, together with the results from Hopkins & Archer (2014) as well as the results from 4 previously unpublished microcosm experiments from the NW European shelf cruise and a

350   further 2 temperate water microcosm experiments from the Arctic cruise (*North Sea* and *Iceland Basin*, Table 1). This gives a total of 18 microcosm experiments, each with between 1 and 3 high CO_2 treatments.

Hopkins & Archer (2014) reported consistent and significant increases in DMS concentration in response to elevated CO_2 that were accompanied by significant decreases in DMSPt

355   concentrations. Bacterially-mediated DMS processes appeared to be insensitive to OA, with no detectable effects on dark rates of DMS consumption and gross production, and no consistent response seen in bacterial abundance (Hopkins and Archer 2014). In general, there were large short-term decreases in Chl *a* concentrations and phototrophic nanoflagellate abundance in response to elevated CO_2 in these experiments (Richier et al. 2014).

360   The relative treatment effects ($[x]_{highCO2}/[x]_{ambientCO2}$) for DMS and DMSP (Figure 6), Chl a,

phototrophic nanoflagellate abundance and relative growth rates (Figure 7) are plotted

against the ratio of DIC to total alkalinity (DIC/Alk) of the sampled waters, in order to place

our findings in context of the total experimental data set. The value of DIC/Alk ranges from

0.84 – 0.95 within the mixed layer, and increases towards high latitude waters (Egleston et al.

365   2010). Thus, stations with DIC/Alk above ~0.91 represent the seven polar stations (right of

red dashed line Fig. 6 and 7). The surface waters of the polar oceans have a reduced

buffering capacity due to higher CO_2 solubility in colder waters, and so are less resistant to

local variations in DIC and Alk (Sabine et al. 2004). Thus, the relationship between

experimental response and DIC/Alk is a simple way of demonstrating how the CO_2

370   sensitivity of different surface ocean communities relates to the *in situ* carbonate chemistry.

The effect of elevated CO_2 on DMS concentrations at polar stations, relative to ambient

controls, was minimal at both T_1 and T_2, and is in strong contrast to the results from identical

experiments performed on the NW European shelf. At temperate stations, DMSP displayed a

clear negative treatment effect, whilst at polar stations a positive effect was evident under

375   high CO_2, and particularly at T_1 (Fig. 6 C and D). *De novo* DMSP synthesis and DMSP

production rates show a similar relationship with DIC/Alk (Fig. 7 A and B), with a tendency

towards suppression of these rates in temperate waters at elevated CO_2 and a tendency

towards a positive effect in polar waters. However, the smaller number of data makes the

relationships less definitive. At T_1, Chl a showed little response to elevated CO_2 at polar

380   stations, whereas a strong negative response was seen in temperate waters (Fig. 8A). A slight

positive response in Chl a was seen at most temperate stations by T_2, with generally little

response at polar stations (Fig. 8 B).

In general, phototrophic nanoflagellates responded to high CO_2 with large decreases in

abundance in temperate waters (Richier et al. 2014), and increases in abundance in polar

385 waters (Fig. 8 C and D), with some exceptions: *North Sea* and *South Sandwich* gave the

opposite response. The impacts had lessened by T_2. In contrast, bacterial abundance did not

show the same regional differences in response to high CO_2 (see Hopkins and Archer (2014)

for temperate waters, and Figure S1, supplementary information, for polar waters). Bacterial

abundance in temperate waters gave variable and inconsistent responses to high CO_2. For all

390 Arctic stations, *Drake Passage* and *Weddell Sea*, no response to high CO_2 was observed. For

South Georgia and *South Sandwich*, bacterial abundance increased at 1000 and 2000 μatm,

with significant increases for *South Georgia* after 144 h of incubation (ANOVA $F = 137.936$,

$p<0.001$).

The treatment effect on relative growth rate (RGR) (Fig. 8 E and F) at T_1 was minimal across

395 all stations, with the exception of some outliers. Treatment effects were more discernible by

T_2, with a strong negative impact in temperate waters, contrasting with a minimal to positive

effect at polar stations. Additionally, at Arctic stations *Greenland Gyre* and *Greenland Ice-*

edge, no overall effect of increased CO_2 on rates of DOC release, total carbon fixation or

POC : DOC was observed (Poulton et al. 2016).

400 In summary, the relative response in both DMS(P) and a range of biological parameters to

CO_2 treatment in polar waters follows a distinctly different pattern to experiments performed

in temperate waters. In the following sections we explore the possible drivers of the regional

variability in response to OA.

4.2 Influence of community cell-size composition on DMS response

405 It has been proposed that variability in the concentrations of carbonate species (e.g. pCO_2,

HCO_3^-, CO_3^{2-}) experienced by phytoplankton is related to cell size, such that smaller-celled

taxa (<10 μm) with a reduced diffusive boundary layer are naturally exposed to relatively less

variability compared to larger cells (Flynn et al. 2012). Thus, short-term and rapid changes in

carbonate chemistry, such as the kind imposed during our microcosm experiments, may have

410   a disproportionate effect on the physiology and growth of smaller celled species. Larger cells

may be better able to cope with variability as normal cellular metabolism results in significant

cell surface changes in carbonate chemistry parameters (Richier et al. 2014). Indeed, the

marked response in DMS concentrations to short term OA in temperate waters has been

attributed to this enhanced sensitivity of small phytoplankton (Hopkins and Archer 2014).

415   Was the lack of DMS response to OA in polar waters therefore a result of the target

communities being dominated by larger-celled, less carbonate-sensitive species?

Size-fractionated Chl *a* measurements give an indication of the relative contribution of large

and small phytoplankton cells to the community. For experiments in temperate waters, the

mean ratio of >10 µm Chl *a* to total Chl *a* (hereafter *>10 µm : total*) of 0.32 ± 0.08 was lower

420   than the ratio for polar stations of 0.54 ± 0.13 (Table 2). Although the difference was not

statistically significant, this might imply a tendency towards communities dominated by

larger cells in the polar oceans, which may partially explain the apparent lack of DMS

response to elevated CO_2. However, this is not a consistent explanation for the observed

responses. For example, the Arctic *Barents Sea* station had the lowest observed *>10 µm :*

425   *total* of 0.04 ± 0.01, suggesting a community comprised almost entirely of <10 µm cells; yet

the response to short term OA differed to the response seen in temperate waters. No

significant CO_2 effects on DMS or DMSP concentrations or production rates were observed

at this station, whilst total Chl *a* significantly increased under the highest CO_2 treatments

after 96 h (PERMANOVA $F = 33.239$, $P<0.001$). Thus, our cell size theory does not hold for

430   all polar waters, suggesting that regardless of the dominant cell size, polar communities are

more resilient to OA. In the following section, we explore the causes of this apparent

resilience in terms of the environmental conditions to which the communities have

presumably adapted.

4.3 Adaptation to a variable carbonate chemistry environment

435   The variation in *in situ* surface ocean carbonate chemistry parameters for all three cruises (see

Tynan et al. 2016 for details), is summarised in Figure 9. These data demonstrate both the

latitudinal differences in surface ocean carbonate chemistry between temperate and polar

waters, as well as the within-region variability which is controlled by the respective buffer

capacities. Thus, a narrow range of values for all carbonate parameters was observed in the

440   NW European shelf waters relative to the less well-buffered Arctic and Southern Ocean

waters. The polar waters sampled during our study were characterised by pronounced

gradients in carbonate chemistry over small spatial scales, such that surface ocean

communities are more likely to have experienced fluctuations between high $pH/\Omega_{aragonite}$ and

low $pH/\Omega_{aragonite}$ over short time scales (Tynan et al. 2016). For example, pH_T varied by only

445   0.15 units (8.20 - 8.05) in NW European shelf waters, compared to 0.35 units (8.05 - 7.7) in

the Arctic, and 0.40 units (8.25 - 7.85) in the Southern Ocean. Our data represent only a

snapshot (4 – 6 weeks) of a year, so the annual variability in carbonate chemistry is likely to

be much greater. Adaptation to such natural variability may induce resilience to abrupt

changes within the biological community (Kapsenberg et al. 2015). This resilience is

450   manifested here as negligible impacts on rates of *de novo* DMSP synthesis and net DMS

production. The few published studies in polar waters have reported similar findings.

Phytoplankton communities were able to tolerate a pCO_2 range of 84 – 643 µatm in ~12 d

minicosm experiments (650 L) in Antarctic coastal waters, with no effects on

nanophytoplankton abundance, and enhanced abundance of picophytoplankton and

455   prokaryotes (Davidson et al. 2016; Thomson et al. 2016). In experiments under the Arctic ice,

microbial communities demonstrated the capacity to respond either by selection or

physiological plasticity to elevated CO_2 during short term experiments (Monier et al. 2014).

Our findings support the notion that, relative to temperate communities, polar microbial

communities are already adapted to, and are able to tolerate, large variations in carbonate

460   chemistry. Thus by performing multiple, highly replicated experiments over a broad

geographic range, the findings of this study imply that the DMS response may be both a

reflection of: (i) the level of sensitivity of the community to changes in the mean state of

carbonate chemistry, and (ii) the levels of regional variability in carbonate chemistry

experienced by different communities. This highlights the limitations associated with simple

465   extrapolation of results from a small number of geographically-limited experiments e.g. Six

et al. (2013). Such an approach lacks a mechanistic understanding that would allow a model

to capture the regional variability in response that is apparent from the microcosms

experiments presented here.

4.4 Comparison to an Arctic mesocosm experiment

470   The DMS responses to OA within our short term microcosm experiments contrast with the

results of an earlier Arctic mesocosm experiment (Archer et al. 2013). Whilst no response in

DMS concentrations to OA was generally seen in the microcosm experiments discussed here,

a significant decrease in DMS with increasing levels of CO_2 in the earlier mesocosm study

was reported. We now explore and consider the reasons behind these differences.

475   The short duration of the microcosm experiments (maximum of 4 – 7 d) allows the

physiological (phenotypic) capacity of the community to changes in carbonate chemistry to

be assessed. In other words, how well is the community adapted to variable carbonate

chemistry and how does this influence its ability to acclimate to change? Although the

mesocosm experiment considered a longer time period (4 weeks), the first few days can be

480   compared to the microcosms. No differences in DMS or DMSP concentrations were detected

for the first week of the mesocosm experiment, implying a certain level of insensitivity of

DMS production to the rapid changes in carbonate chemistry. In fact, when taking all

previous mesocosm experiments into consideration, differences in DMS concentrations have

consistently been undetectable during the first 5 – 10 days, implying there is a limited short-

485   term physiological response by the in situ communities (Vogt et al. 2008; Hopkins et al.

2010; Kim et al. 2010; Avgoustidi et al. 2012; Park et al. 2014). This is in contrast to the

strong response in the temperate microcosms from the NW European shelf (Hopkins and

Archer 2014). However, all earlier mesocosm experiments have been performed in coastal

waters, which like polar waters, can experience a large natural range in carbonate chemistry.

490   In the case of coastal waters this is driven to a large extent by the influence of riverine

discharge and biological activity (Fassbender et al. 2016). Thus coastal communities may

also possess a higher level of adaptation to variable carbonate chemistry compared to the

open ocean communities of the temperate microcosms reported here (Fassbender et al. 2016).

The later stages of mesocosm experiments address a different set of hypotheses, and are less

495   comparable to the microcosms reported here. With time, an increase in number of generations

leads to community structure changes and taxonomic shifts, driven by selection on the

standing genetic variation in response to the altered conditions. Moreover, the coastal Arctic

mesocosms were enriched with nutrients after 10 days, and the resultant relief from nutrient

limitation allowed differences between pCO$_2$ treatments to be exposed, including a strong

500   DMS(P) response (Archer et al. 2013; Schulz et al. 2013). During this period of increased

growth and productivity, CO$_2$ increases drove changes which reflected both the physiological

and genetic potential within the community, and resulted in taxonomic shifts. The resultant

population structure was changed, with an increase in abundance of dinoflagellates,

particularly *Heterocapsa rotundata*. Increases in DMSP concentrations and DMSP synthesis

505   rates were attributed to the population shift towards dinoflagellates. The drivers of the

reduced DMS concentrations were less clear, but may have been linked to reduced DMSP-

lyase capacity within the dominant phytoplankton, a reduction in bacterial DMSP lysis, or an

increase in bacterial DMS consumption rates (Archer et al. 2013). Again, this is comparable

to all other mesocosm experiments, wherein changes to DMS concentrations can be

510 associated with CO_2-driven shifts in community structure (Vogt et al. 2008; Hopkins et al.

2010; Kim et al. 2010; Avgoustidi et al. 2012; Park et al. 2014; Webb et al. 2015). However,

given the lack of further experiments of a similar location, design and duration to the Arctic

mesocosm, it is unclear how representative the mesocosm result is of the general community-

driven response to OA in high latitude waters.

515 As expected, given the shorter duration of the microcosms, we did not generally see any

broad-scale CO_2-effects on community structure in polar waters. This can be demonstrated by

a lack of significant differences in the mean ratio of >10 μm Chl *a* to total Chl *a* (*>10 μm :*

total) between CO_2 treatments, implying there were no broad changes in community

composition (Table 2). *South Sandwich* was an exception to this, where large and significant

520 increases in the mean ratio of *>10 μm : total* were observed at 750 μatm and 2000 μatm CO_2

relative to ambient CO_2 (ANOVA, $F = 207.144$, $p<0.001$, $df = 3$). Interestingly, this was also

the only polar station that exhibited any significant effects on DMS after 96 h of incubation

(Figure 3G). However, given the lack of similar response at 1000 μatm, it remains equivocal

whether this was driven by a CO_2-effect or some other factor. The results of our microcosm

525 experiments suggest resilience in *de novo* DMSP production and net DMS production in the

microbial communities of the polar open oceans in response to short term changes in

carbonate chemistry. This may be driven by a high level of adaptation within the targeted

phytoplankton communities to naturally varying carbonate chemistry.

In contrast to our findings, a recent single 9 day microcosm experiment (Hussherr et al.,

530 2017) performed in Baffin Bay (Canadian Arctic) saw a 25% decrease in DMS

concentrations during spring bloom-like conditions. This implies that polar DMS production

may be sensitive to OA at certain times of the year, such as during the highly productive

spring bloom, but less sensitive during periods of stable productivity, such as the summer

months sampled during this study. This emphasises the need to gain a more detailed

535   understanding of both the spatial and seasonal variability in the polar DMS response to

changing ocean acidity.

5 Conclusions

We have shown that net DMS production by summertime polar open ocean microbial

communities is resilient to OA during multiple, highly replicated short term microcosm

540   experiments. We provide further evidence that, in contrast to temperate communities

(Hopkins and Archer 2014), polar communities we sampled were relatively insensitive to

variations in carbonate chemistry (Davidson et al. 2016; Richier et al. under review),

manifested here as a minimal effect on net DMS production. Our findings contrast with two

previous studies performed in coastal Arctic waters (Archer et al. 2013, Hussherr et al. 2017)

545   which showed significant decreases in DMS in response to OA. These discrepancies may be

driven by differences in the sensitivity of microbial communities to changing carbonate

chemistry between coastal and open ocean waters, or by variability in the response to OA

depending on the time of year, nutrient availability, and ambient levels of growth and

productivity. This serves to highlight the complex spatial and temporal variability in DMS

550   response to OA which warrants further investigation to improve model predictions.

Our findings should be considered in the context of timescales of change (experimental vs

real world OA) and the potential of microbial communities to adapt to a gradually changing

environment. Microcosm experiments focus on the physiological response of microbial

communities to short term OA. Mesocosm experiments consider a timescale that allows the

555   response to be driven by community composition shifts, but are not long enough in duration

to incorporate an adaptive response. Neither approach is likely to accurately simulate the

response to the gradual changes in surface ocean pH that will occur over the next 50 – 100 years, nor the resulting changes in microbial community structure and distribution. However, results from our study indicate that the DMS response to OA should be considered not only in

560   relation to experimental perturbations to carbonate chemistry, but also in relation to the magnitude of background variability in carbonate chemistry experienced by the DMS-producing organisms and communities. Our findings suggest a strong link between the DMS response to OA and background regional variability in the carbonate chemistry.

Models suggest the climate may be sensitive to changes in the spatial distribution of DMS

565   emissions over global scales (Woodhouse et al. 2013). Such changes could be driven by both physiological and adaptive responses to environmental change. Accepting the limitations of experimental approaches, our findings suggest that net DMS production from polar oceans may be resilient to OA in the context of its short term effects on microbial communities. The oceans face a multitude of CO_2-driven changes in the coming decades, including OA,

570   warming, deoxygenation and loss of sea ice (Gattuso et al. 2015). Our study addresses only one aspect of these future ocean stressors, but contributes to our understanding of how DMS emissions from the polar oceans may alter, facilitating a better understanding of Earth's future climate.

Acknowledgements

575   This work was funded under the UK Ocean Acidification thematic programme (UKOA) via the UK Natural Environment Research Council (NERC) grants to PD Nightingale and SD Archer (NE/H017259/1) and to T Tyrell, EP Achterberg and CM Moore (NE/H017348/1). The UK Department for Environment, Food and Rural Affairs (Defra) and the UK Department of Energy and Climate Change (DECC) also contributed to funding UKOA. The

580   National Science Foundation, United States, provided additional support to SD Archer ((NSF

OCE-1316133). Our work and transit in the coastal waters of Greenland, Iceland and

Svalbard was granted thanks to permissions provided by the Danish, Icelandic and

Norwegian diplomatic authorities. We thank the captains and crew of the RRS Discovery

(cruise D366) and RRS James Clark Ross (cruises JR271 and JR274), and the technical staff

585   of the National Marine Facilities and the British Antarctic Survey. We are grateful to Mariana

Ribas-Ribas and Eithne Tynan for carbonate chemistry data, Elaine Mitchell and Clement

Georges for flow cytometry data, and Mariana Ribas-Ribas and Rob Thomas (BODC) for

data management.

References

590   Archer, S. D., S. A. Kimmance, J. A. Stephens, F. E. Hopkins, R. G. J. Bellerby, K. G.
Schulz, J. Piontek and A. Engel (2013). "Contrasting responses of DMS and DMSP to ocean
acidification in Arctic waters." Biogeosciences **10**(3): 1893-1908.

Avgoustidi, V., P. D. Nightingale, I. R. Joint, M. Steinke, S. M. Turner, F. E. Hopkins and P.
595   S. Liss (2012). "Decreased marine dimethyl sulfide production under elevated CO_2 levels in
mesocosm and in vitro studies." Environmental Chemistry **9**(4): 399-404.

Bigg, E. K. and C. Leck (2001). "Properties of the aerosol over the central Arctic Ocean."
Journal of Geophysical Research: Atmospheres **106**(D23): 32101-32109.

600
Brussaard, C. P. D., A. A. M. Noordeloos, H. Witte, M. C. J. Collenteur, K. Schulz, A.
Ludwig and U. Riebesell (2013). "Arctic microbial community dynamics influenced by
elevated CO_2 levels." Biogeosciences **10**(2): 719-731.

605   Carpenter, L. J., S. D. Archer and R. Beale (2012). "Ocean-atmosphere trace gas exchange."
Chemical Society Reviews **41**(19): 6473-6506.

Chang, R. Y. W., S. J. Sjostedt, J. R. Pierce, T. N. Papakyriakou, M. G. Scarratt, S. Michaud,
M. Levasseur, W. R. Leaitch and J. P. Abbatt (2011). "Relating atmospheric and oceanic
610   DMS levels to particle nucleation events in the Canadian Arctic." Journal of Geophysical
Research: Atmospheres **116**(D17).

Charlson, R. J., J. E. Lovelock, M. O. Andreae and S. G. Warren (1987). "Oceanic
phytoplankton, atmospheric sulphur, cloud albedo and climate." Nature **326**: 655-661.

615

Chen, T. and M. Jang (2012). "Secondary organic aerosol formation from photooxidation of a mixture of dimethyl sulfide and isoprene." Atmospheric Environment **46**: 271-278.

620   Crawfurd, K. J., C. P. D. Brussaard and U. Riebesell (2016). "Shifts in the microbial community in the Baltic Sea with increasing CO2." Biogeosciences Discuss. **2016**: 1-51.

Davidson, A. T., J. McKinlay, K. Westwood, P. Thompson, R. van den Enden, M. de Salas, S. Wright, R. Johnson and K. Berry (2016). "Enhanced CO 2 concentrations change the structure of Antarctic marine microbial communities." Mar Ecol Prog Ser. doi **10**: 3354.

625

Egleston, E. S., C. L. Sabine and F. M. M. Morel (2010). "Revelle revisited: Buffer factors that quantify the response of ocean chemistry to changes in DIC and alkalinity." Global Biogeochemical Cycles **24**(1): n/a-n/a.

630   Engel, A., K. Schulz, U. Riebesell, R. Bellerby, B. Delille and M. Schartau (2008). "Effects of CO_2 on particle size distribution and phytoplankton abundance during a mesocosm bloom experiment (PeECE II)." Biogeosciences **5**: 509-521.

Engel, A., I. Zondervan, K. Aerts, L. Beaufort, A. Benthien, L. Chou, B. Delille, J.-P.
635   Gattuso, J. Harlay, C. Heeman, L. Hoffman, S. Jacquet, J. Nejstgaard, M.-D. Pizay, E. Rochelle-Newall, U. Schneider, A. Terbrueggen and U. Riebesell (2005). "Testing the direct effect of CO_2 concentrations on a bloom of the coccolithophorid *Emiliania huxleyi* in mesocosm experiments." Limnology and Oceanography **50**(2): 493-507.

640   Fassbender, A. J., C. L. Sabine and K. M. Feifel (2016). "Consideration of coastal carbonate chemistry in understanding biological calcification." Geophysical Research Letters **43**(9): 4467-4476.

Flynn, K. J., J. C. Blackford, M. E. Baird, J. A. Raven, D. R. Clark, J. Beardall, C. Brownlee,
645   H. Fabian and G. L. Wheeler (2012). "Changes in pH at the exterior surface of plankton with ocean acidification." Nature Climate Change **2**(7): 510-513.

Gabric, A. J., B. Qu, P. A. Matrai, C. Murphy, H. Lu, D. R. Lin, F. Qian and M. Zhao (2014). "Investigating the coupling between phytoplankton biomass, aerosol optical depth and sea-ice
650   cover in the Greenland Sea." Dynamics of Atmospheres and Oceans **66**(0): 94-109.

Gattuso, J.-P., K. Lee, B. Rost and K. Schulz (2010). Approaches and tools to manipulate the carbonate chemistry. Guide to Best Practices for Ocean Acidification Research and Data Reporting. U. Riebesell, V. J. Fabry, L. Hansson and J. P. Gattuso. Pulblications Office of the
655   European Union, Luxembourg**:** 263.

Gattuso, J.-P., A. Magnan, R. Bille, W. Cheung, E. Howes, F. Joos, D. Allemand, L. Bopp, S. Cooley and C. Eakin (2015). "Contrasting futures for ocean and society from different anthropogenic CO2 emissions scenarios." Science **349**(6243): aac4722.

660

Hönisch, B., A. Ridgwell, D. N. Schmidt, E. Thomas, S. J. Gibbs, A. Sluijs, R. Zeebe, L. Kump, R. C. Martindale, S. E. Greene, W. Kiessling, J. Ries, J. C. Zachos, D. L. Royer, S. Barker, T. M. Marchitto, R. Moyer, C. Pelejero, P. Ziveri, G. L. Foster and B. Williams (2012). "The Geological Record of Ocean Acidification." Science **335**(6072): 1058-1063.

665

Hopkins, F. E. and S. D. Archer (2014). "Consistent increase in dimethyl sulfide (DMS) in response to high CO2 in five shipboard bioassays from contrasting NW European waters." Biogeosciences **11**(18): 4925-4940.

670 Hopkins, F. E., S. M. Turner, P. D. Nightingale, M. Steinke, D. Bakker and P. S. Liss (2010). "Ocean acidification and marine trace gas emissions." Proceedings of the National Academy of Sciences **107**(2): 760-765.

Hopkins, F. E., S. M. Turner, P. D. Nightingale, M. Steinke and P. S. Liss (2010). "Ocean
675 acidification and marine biogenic trace gas production." Proceedings of the National Academy of Sciences **107**(2): 760-765.

Hussherr, R., M. Levasseur, M. Lizotte, J.-É. Tremblay, J. Mol, T. Helmuth, M. Gosselin, M. Starr, L. A. Miller and T. Jarniková (2017). "Impact of ocean acidification on Arctic
680 phytoplankton blooms and dimethyl sulfide concentration under simulated ice-free and under-ice conditions." Biogeosciences **14**(9): 2407.

Jarníková, T. and P. D. Tortell (2016). "Towards a revised climatology of summertime dimethylsulfide concentrations and sea–air fluxes in the Southern Ocean." Environmental
685 Chemistry **13**(2): 364-378.

Johnson, M. T. and T. G. Bell (2008). "Coupling between dimethylsulfide emissions and the ocean-atmosphere exchange of ammonia." Environmental Chemistry **5**(4): 259-267.

690 Kapsenberg, L., A. L. Kelley, E. C. Shaw, T. R. Martz and G. E. Hofmann (2015). "Near-shore Antarctic pH variability has implications for the design of ocean acidification experiments." Scientific Reports **5**: 9638.

Kiene, R. P. and D. Slezak (2006). "Low dissolved DMSP concentrations in seawater
695 revealed by small-volume gravity filtration and dialysis sampling " Limnology and Oceanography Methods **4**: 80-95.

Kim, J. M., K. Lee, K. Shin, J. H. Kang, H. W. Lee, M. Kim, P. G. Jang and M. C. Jang (2006). "The effect of seawater CO2 concentration on growth of a natural phytoplankton

700   assemblage in a controlled mesocosm experiment." Limnology and Oceanography **51**(4):
        1629-1636.

        Kim, J. M., K. Lee, E. J. Yang, K. Shin, J. H. Noh, K. T. Park, B. Hyun, H. J. Jeong, J. H.
        Kim, K. Y. Kim, M. Kim, H. C. Kim, P. G. Jang and M. C. Jang (2010). "Enhanced
705   Production of Oceanic Dimethylsulfide Resulting from CO2-Induced Grazing Activity in a
        High CO2 World." Environmental Science & Technology **44**(21): 8140-8143.

        Korhonen, H., K. S. Carslaw, D. V. Spracklen, G. W. Mann and M. T. Woodhouse (2008).
        "Influence of oceanic dimethyl sulfide emissions on cloud condensation nuclei concentrations
710   and seasonality over the remote Southern Hemisphere oceans: A global model study." Journal
        of Geophysical Research-Atmospheres **113**(D15): 16.

        Korhonen, H., K. S. Carslaw, D. V. Spracklen, D. A. Ridley and J. Ström (2008). "A global
        model study of processes controlling aerosol size distributions in the Arctic spring and
715   summer." Journal of Geophysical Research **113**(D8): D08211.

        Lana, A., T. G. Bell, R. Simó, S. M. Vallina, J. Ballabrera-Poy, A. J. Kettle, J. Dachs, L.
        Bopp, E. S. Saltzman, J. Stefels, J. E. Johnson and P. S. Liss (2011). "An updated
        climatology of surface dimethylsulfide concentrations and emission fluxes in the global
720   ocean." Global Biogeochem. Cycles **25**(1): GB1004.

        Leaitch, W. R., S. Sharma, L. Huang, D. Toom-Sauntry, A. Chivulescu, A. M. Macdonald, K.
        von Salzen, J. R. Pierce, A. K. Bertram and J. C. Schroder (2013). "Dimethyl sulfide control
        of the clean summertime Arctic aerosol and cloud." Elementa: Science of the Anthropocene
725   **1**(1): 000017.

        Levasseur, M. (2013). "Impact of Arctic meltdown on the microbial cycling of sulphur."
        Nature Geoscience **6**(9): 691-700.

730   Lewis, E. and D. W. R. Wallace (1998). Program Developed for CO2 System Calculations.
        Carbon Dioxide Information Analysis Center, Oak Ridge National Laboratory, U.S.
        Department of Energy, Oak Ridge, Tennessee.

        McCoy, D. T., S. M. Burrows, R. Wood, D. P. Grosvenor, S. M. Elliott, P.-L. Ma, P. J. Rasch
735   and D. L. Hartmann (2015). "Natural aerosols explain seasonal and spatial patterns of
        Southern Ocean cloud albedo." Science Advances **1**(6).

        McNeil, B. I. and R. J. Matear (2008). "Southern Ocean acidification: A tipping point at 450-
        ppm atmospheric CO2." Proceedings of the National Academy of Sciences **105**(48): 18860-
740   18864.

Monier, A., H. S. Findlay, S. Charvet and C. Lovejoy (2014). "Late winter under ice pelagic microbial communities in the high Arctic Ocean and the impact of short-term exposure to elevated CO2 levels." Name: Frontiers in Microbiology **5**: 490.

745

Orr, J. C., V. J. Fabry, O. Aumont, L. Bopp, S. C. Doney, R. A. Feely, A. Gnanadesikan, N. Gruber, A. Ishida and F. Joos (2005). "Anthropogenic ocean acidification over the twenty-first century and its impact on calcifying organisms." Nature **437**(7059): 681-686.

750   Park, K.-T., K. Lee, K. Shin, E. J. Yang, B. Hyun, J.-M. Kim, J. H. Noh, M. Kim, B. Kong, D. H. Choi, S.-J. Choi, P.-G. Jang and H. J. Jeong (2014). "Direct Linkage between Dimethyl Sulfide Production and Microzooplankton Grazing, Resulting from Prey Composition Change under High Partial Pressure of Carbon Dioxide Conditions." Environmental Science & Technology **48**(9): 4750-4756.

755

Petters, M. D. and S. M. Kreidenweis (2007). "A single parameter representation of hygroscopic growth and cloud condensation nucleus activity." Atmos. Chem. Phys. **7**(8): 1961-1971.

760   Poulton, A. J., C. J. Daniels, M. Esposito, M. P. Humphreys, E. Mitchell, M. Ribas-Ribas, B. C. Russell, M. C. Stinchcombe, E. Tynan and S. Richier (2016). "Production of dissolved organic carbon by Arctic plankton communities: Responses to elevated carbon dioxide and the availability of light and nutrients." Deep Sea Research Part II: Topical Studies in Oceanography **127**: 60-74.

765

Raven, J., K. Caldeira, H. Elderfield, O. Hoegh-Guldberg, P. Liss, U. Riebesell, J. Shepherd, C. Turley and A. Watson (2005). "Ocean acidification due to increasing atmospheric carbon dioxide." The Royal Society **Policy Document 12/05, London**.

770   Rempillo, O., A. M. Seguin, A. L. Norman, M. Scarratt, S. Michaud, R. Chang, S. Sjostedt, J. Abbatt, B. Else and T. Papakyriakou (2011). "Dimethyl sulfide air-sea fluxes and biogenic sulfur as a source of new aerosols in the Arctic fall." Journal of Geophysical Research: Atmospheres **116**(D17).

775   Richier, S., E. P. Achterberg, C. Dumousseaud, A. J. Poulton, D. J. Suggett, T. Tyrrell, M. V. Zubkov and C. M. Moore (2014). "Phytoplankton responses and associated carbon cycling during shipboard carbonate chemistry manipulation experiments conducted around Northwest European shelf seas." Biogeosciences **11**(17): 4733-4752.

780   Richier, S., E. P. Achterberg, M. P. Humphreys, A. J. Poulton, D. J. Suggett, T. Tyrrell and C. M. Moore (under review). "Geographical CO_2 sensitivity of phytoplankton correlates with ocean buffer capacity." Global Change Biology.

785   Riebesell, U., J. P. Gattuso, T. F. Thingstad and J. J. Middelburg (2013). "Preface "Arctic ocean acidification: pelagic ecosystem and biogeochemical responses during a mesocosm study"." Biogeosciences **10**(8): 5619-5626.

Sabine, C. L., R. A. Feely, N. Gruber, R. M. Key, K. Lee, J. L. Bullister, R. Wanninkhof, C. S. Wong, D. W. R. Wallace, B. Tilbrook, F. J. Millero, T.-H. Peng, A. Kozyr, T. Ono and A.
790   F. Rios (2004). "The oceanic sink for anthropogenic CO_2." Science **305**: 367-371.

Schoemann, V., S. Becquevort, J. Stefels, V. Rousseau and C. Lancelot (2005). "Phaeocystis blooms in the global ocean and their controlling mechanisms: a review." Journal of Sea Research **53**(1): 43-66.

795
Schulz, K. G., R. G. J. Bellerby, C. P. D. Brussaard, J. Büdenbender, J. Czerny, A. Engel, M. Fischer, S. Koch-Klavsen, S. A. Krug, S. Lischka, A. Ludwig, M. Meyerhöfer, G. Nondal, A. Silyakova, A. Stuhr and U. Riebesell (2013). "Temporal biomass dynamics of an Arctic plankton bloom in response to increasing levels of atmospheric carbon dioxide."
800   Biogeosciences **10**(1): 161-180.

Schulz, K. G., U. Riebesell, R. G. J. Bellerby, H. Biswas, M. Meyerhofer, M. N. Muller, J. K. Egge, J. C. Nejstgaard, C. Neill, J. Wohlers and E. Zollner (2008). "Build-up and decline of organic matter during PeECE III." Biogeosciences **5**: 707-718.

805
Sharma, S., E. Chan, M. Ishizawa, D. Toom-Sauntry, S. Gong, S. Li, D. Tarasick, W. Leaitch, A. Norman and P. Quinn (2012). "Influence of transport and ocean ice extent on biogenic aerosol sulfur in the Arctic atmosphere." Journal of Geophysical Research: Atmospheres **117**(D12).

810
Six, K. D., S. Kloster, T. Ilyina, S. D. Archer, K. Zhang and E. Maier-Reimer (2013). "Global warming amplified by reduced sulphur fluxes as a result of ocean acidification." Nature Climate Change **3**(11): 975.

815   Stefels, J. (2000). "Physiological aspects of the production and conversion of DMSP in marine algae and higher plants." Journal of Sea Research **43**: 183-197.

Steinacher, M., F. Joos, T. L. Frolicher, G. K. Plattner and S. C. Doney (2009). "Imminent ocean acidification in the Arctic projected with the NCAR global coupled carbon cycle-
820   climate model." Biogeosciences **6**(4): 515-533.

Stillman, J. H. and A. W. Paganini (2015). "Biochemical adaptation to ocean acidification." Journal of Experimental Biology **218**(12): 1946-1955.

825   Sunda, W., D. J. Kieber, R. P. Kiene and S. Huntsman (2002). "An antioxidant function for DMSP and DMS in marine algae." Nature **418**: 317-320.

Thomson, P. G., A. T. Davidson and L. Maher (2016). "Increasing CO2 changes community composition of pico- and nano-sized protists and prokaryotes at a coastal Antarctic site." Marine Ecology Progress Series **554**: 51-69.

Tynan, E., J. S. Clarke, M. P. Humphreys, M. Ribas-Ribas, M. Esposito, V. M. C. Rérolle, C. Schlosser, S. E. Thorpe, T. Tyrrell and E. P. Achterberg (2016). "Physical and biogeochemical controls on the variability in surface pH and calcium carbonate saturation states in the Atlantic sectors of the Arctic and Southern Oceans." Deep Sea Research Part II: Topical Studies in Oceanography.

Vogt, M., M. Steinke, S. Turner, A. Paulino, M. Meyerhöfer, U. Riebesell, C. LeQuéré and P. Liss (2008). "Dynamics of dimethylsulphoniopropionate and dimethylsulphide under different CO_2 concentrations during a mesocosm experiment." Biogeosciences **5**: 407-419.

von Glasow, R. and P. J. Crutzen (2004). "Model study of multiphase DMS oxidation with a focus on halogens." Atmos. Chem. Phys. **4**(3): 589-608.

Webb, A. L., E. Leedham-Elvidge, C. Hughes, F. E. Hopkins, G. Malin, L. T. Bach, K. Schulz, K. Crawfurd, C. P. D. Brussaard, A. Stuhr, U. Riebesell and P. S. Liss (2016). "Effect of ocean acidification and elevated fCO2 on trace gas production by a Baltic Sea summer phytoplankton community." Biogeosciences Discuss. **2016**: 1-37.

Webb, A. L., G. Malin, F. E. Hopkins, K. L. Ho, U. Riebesell, K. G. Schulz, A. Larsen and P. S. Liss (2015). "Ocean acidification has different effects on the production of dimethylsulfide and dimethylsulfoniopropionate measured in cultures of Emiliania huxleyi and a mesocosm study: a comparison of laboratory monocultures and community interactions." Environmental Chemistry: -.

Woodhouse, M. T., G. W. Mann, K. S. Carslaw and O. Boucher (2013). "Sensitivity of cloud condensation nuclei to regional changes in dimethyl-sulphide emissions." Atmos. Chem. Phys. **13**(5): 2723-2733.

861 Table 1. Summary of the station locations and characteristic of the water sampled for the 18 microcosm experiments performed in temperate,
862 sub-polar and polar waters.

Cruise	Station ID	Location	Sampling location	Sampling date	Sample depth (m)	SST (°C)	Salinity	Total Chl a (mg/m³)	chl$_{>10\,\mu m}$: chl$_{total}$	pCO_2 (µatm) T_0	pH (total) T_0	Experimental timepoints T_1, T_2 (hours)	Comment
D366	E01	Mingulay Reef	56°47.688N 7°24.300W	8 June 2011	6	11.3	34.8	3.3	no data	334.9	8.1	48, 96	*Hopkins & Archer (2014)*
	E02	Irish Sea	52°28.237N 5°54.052W	14 June 2011	5	11.8	34.4	3.5	0.80 ± 0.03	329.3	8.1	48, 96	*Hopkins & Archer (2014)*
	E02b	Bay of Biscay	46°29.794N 7°12.355W	19 June 2011	5	14.5	35.6	1.8	no data	340.3	8.1	48	*This study*
	E03	Bay of Biscay	46°12.137N 7°13.253W	21 June 2011	10	15.3	35.8	0.8	0.43 ± 0.03	323.9	8.1	48, 96	*Hopkins & Archer (2014)*
	E04	Southern North Sea	52°59.661N 2°29.841E	26 June 2011	5	14.6	34.1	1.3	0.19 ± 0.02	399.8	8.0	48, 96	*Hopkins & Archer (2014)*
	E04b	Mid North Sea	57°45.729N 4°35.434E	29 June 2011	5	13.2	34.8	0.5	0.14 ± 0.003	327.3	8.1	48	*This study*
	E05	Mid North Sea	56°30.293N 3°39.506E	2 July 2011	12	14.0	35.0	0.3	0.23 ± 0.01	360.2	8.1	48, 96	*Hopkins & Archer (2014)*
	E05b	Atlantic Ocean	59°40.721N 4°07.633E	3 July 2011	4	13.4	30.7	0.7	0.12 ± 0.01	310.7	8.1	48	*This study*
	E06	Atlantic Ocean	59°59.011N 2°30.896E	3 July 2011	4	12.5	34.9	1.1	0.14 ± 0.01	287.1	8.2	48	*This study*
JR271	NS	Mid North Sea	56°15.59N 2°37.59E	3 June 2012	15	10.8	35.1	0.3	0.52 ± 0.05	300.5	8.2	48, 96	*This study*
	IB	Iceland Basin	60°35.39N 18°51.23W	8 June 2012	7	10.7	35.2	1.8	0.27 ± 0.02	309.7	8.1	48, 96	*This study*
	GG-AO	Greenland Gyre	76°10.52 N 2°32.96 W	13 June 2012	5	1.7	34.9	1.0	0.34 ± 0.001	289.3	8.2	48, 96	*This study*
	GI-AO	Greenland ice edge	78°21.15 N 3°39.85 W	18 June 2012	5	-1.6	32.6	2.7	0.78 ± 0.03	304.7	8.1	48, 96	*This study*
	BS-AO	Barents Sea	72°53.49 N 26°00.09 W	24 June 2012	5	6.6	35.0	1.3	0.04 ± 0.01	304.3	8.1	48, 96	*This study*
JR274	DP-SO	Drake Passage	58°22.00 S 56°15.12 W	13 Jan 2013	8	1.9	33.2	2.4	1.00 ± 0.06	279.3	8.2	48, 96	*This study*
	WS-SO	Weddell Sea	60°58.55 S 48°05.19 W	18 Jan 2013	6	-1.4	33.6	0.6	0.67 ± 0.06	510.5	7.9	72, 144	*This study*
	SG-SO	South Georgia	52°41.36 S 36°37.28 W	25 Jan 2013	5	2.2	33.9	0.7	0.35 ± 0.04	342.6	8.1	72, 144	*This study*
	SS-SO	South Sandwich	58°05.13 S 25°55.55 W	1 Feb 2013	7	0.5	33.7	4.6	0.57 ± 0.02	272.6	8.2	96, 168	*This study*

863 Table 2. Mean (± SD) ratio of >10μm Chl *a* to total Chl *a* (chl$_{>10\mu m}$:chl$_{total}$) for polar
864 microcosm sampling stations. * indicates significant difference from the response to ambient
865 CO_2.

Station	Time	ambient	550 μatm	750 μatm	1000 μatm	2000 μatm
GG						
	48 h	0.3 ± 0.1	0.3 ± 0.03	0.4 ± 0.2	0.3 ± 0.1	N/A
	96 h	1.0 ± 0.02	0.9 ± 0.2	0.8 ± 0.1	0.7 ± 0.2	
GI						
	48 h	1.0 ± 0.1	1.0 ± 0.1	0.8 ± 0.1	1.0 ± 0.0	N/A
	96 h	1.0 ± 0.1	1.1 ± 0.1	0.8 ± 0.1	0.8 ± 0.1	
BS						
	48 h	0.02 ± 0.01	0.04 ± 0.01	0.03 ± 0.01	0.02 ± 0.01	N/A
	96 h	0.04 ± 0.01	0.05 ± 0.04	0.05 ± 0.04	0.04 ± 0.04	
DP						
	48 h	1.0 ± 0.3	N/A	1.0 ± 0.1	N/A	N/A
	96 h	0.9 ± 0.1		1.0 ± 0.1		
WS						
	72 h	0.6 ± 0.1	N/A	0.7 ± 0.1	N/A	N/A
	144 h	0.7 ± 0.1		0.7 ± 0.1		
SG						
	72 h	0.3 ± 0.02	N/A	0.4 ± 0.1	0.3 ± 0.1	0.4 ± 0.03
	144 h	0.5 ± 0.1		0.6 ± 0.04	0.5 ± 0.1	0.4 ± 0.03
SS						
	96 h	0.7 ± 0.04	N/A	1.5 ± 0.1*	0.7 ± 0.02	1.6 ± 0.1*
	168 h	0.9 ± 0.2		1.4 ± 0.02*	0.8 ± 0.004	1.4 ± 0.2*

866
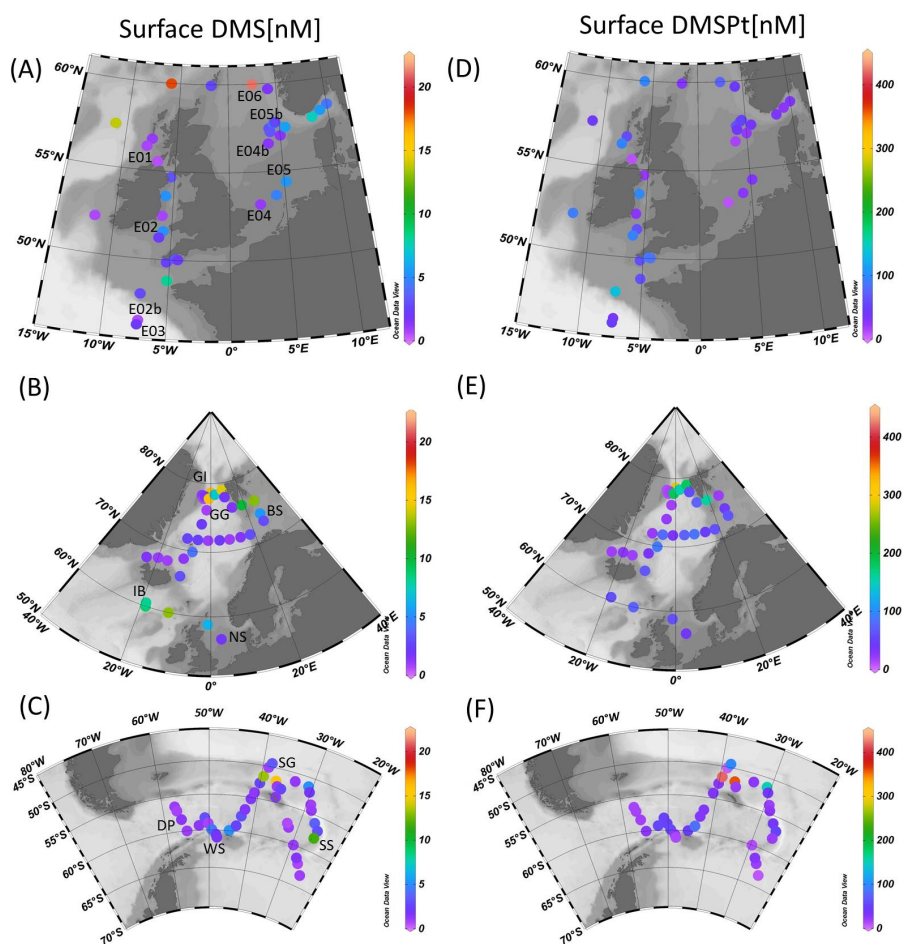
Figure 1. Surface (<5 m) concentrations (nM) of DMS (A-C) and total DMSP (D-F) for
cruises in the NW European shelf (D366) (A,D), the sub-Arctic and Arctic Ocean (JR271)
(B,E) and the Southern Ocean (JR274) (C,F). Locations of sampling stations for microcosm
experiments shown in letters/numbers. E01 – E05: see Hopkins & Archer 2014. NS = *North
Sea*, IB = *Iceland Basin*, GI = *Greenland Ice-edge*, GG = *Greenland Gyre*, BS = *Barents Sea*,
DP = *Drake Passage*, WS = *Weddell Sea*, SG = *South Georgia*, SS = *South Sandwich*.
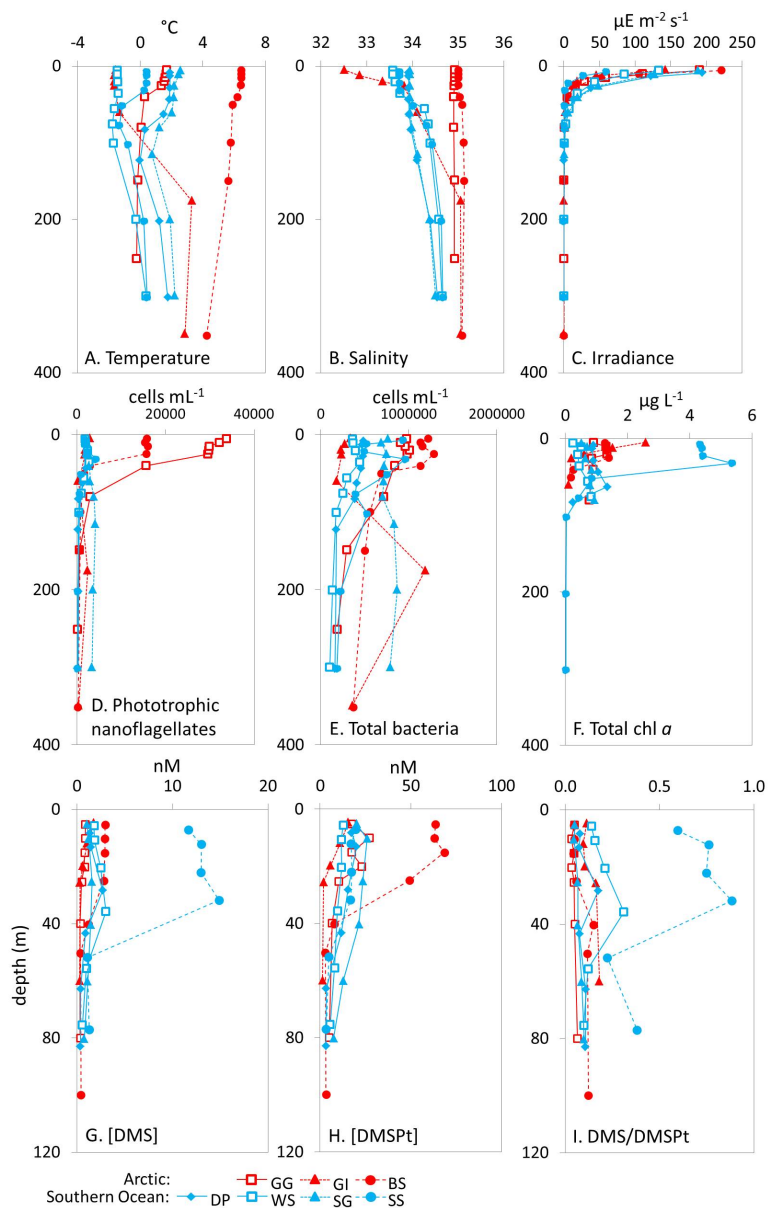
873

874   Figure 2. Depth profiles at the seven polar sampling stations showing A. Temperature (°C),

875   B. Salinity, C. Irradiance ($\mu E\ m^{-2}\ s^{-1}$), D. phototrophic nanoflagellate abundance (cells mL^{-1}),

876   E. total bacteria abundance (cells mL^{-1}), F. total Chl a ($\mu g\ L^{-1}$), G. [DMS] (nM), H. total

877   [DMSP] (nM) and I. DMS/DMSPt from CTD casts at sampling stations for microcosm

878   experiments in Arctic (red) and Southern Ocean (blue) waters. GG = *Greenland Gyre,* GI =

879   *Greenland Ice-edge*, BS = *Barents Sea*, DP = *Drake Passage*, WS = *Weddell Sea*, SG =

880   *South Georgia*, SS = *South Sandwich*

881
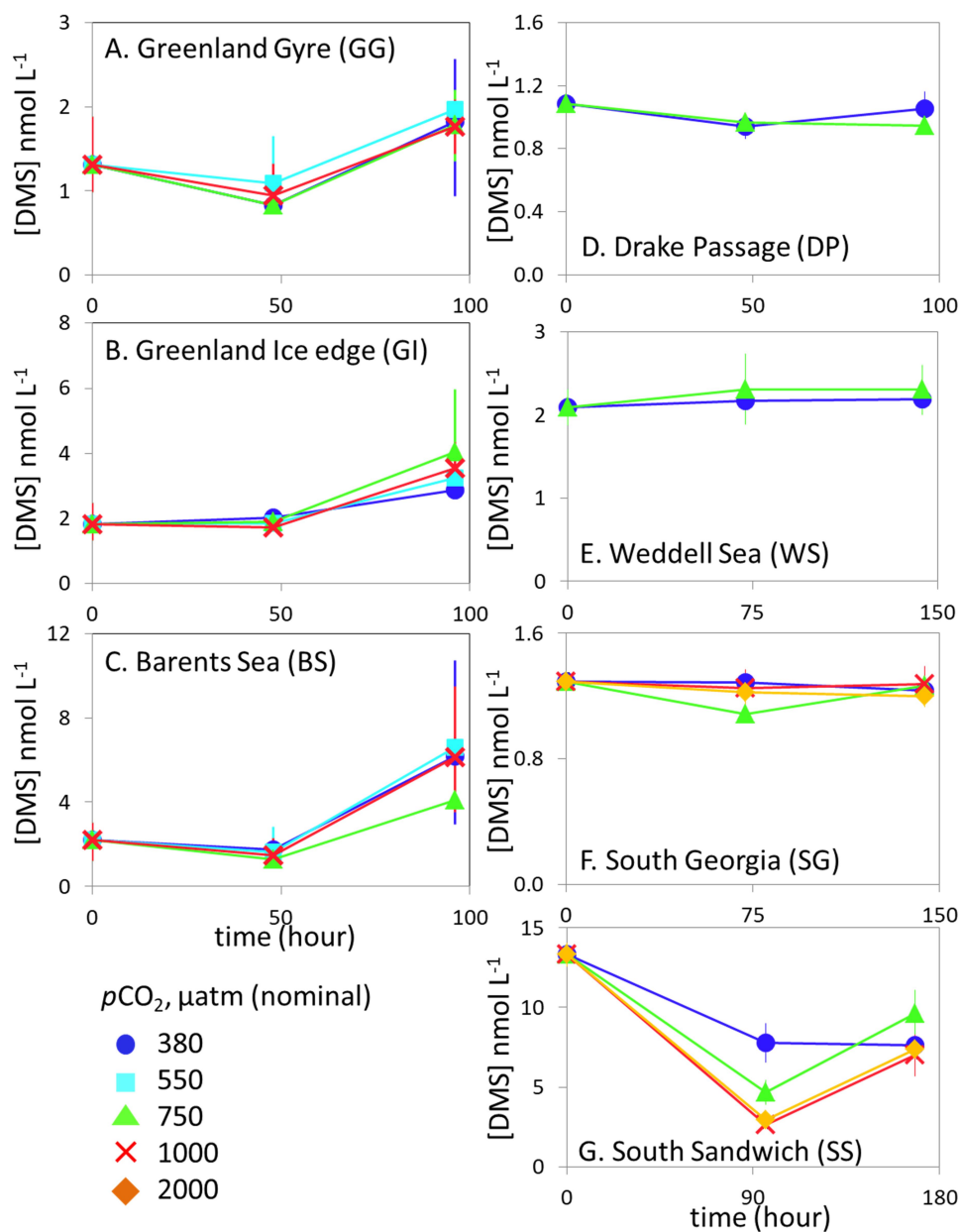
Figure 3. DMS concentrations (nmol L^{-1}) during experimental microcosms performed in
Arctic waters (A - C) and in Southern Ocean waters (D – G). Error bars show standard error.
Locations of water collection for microcosms shown in Figure 1 C – F.

885
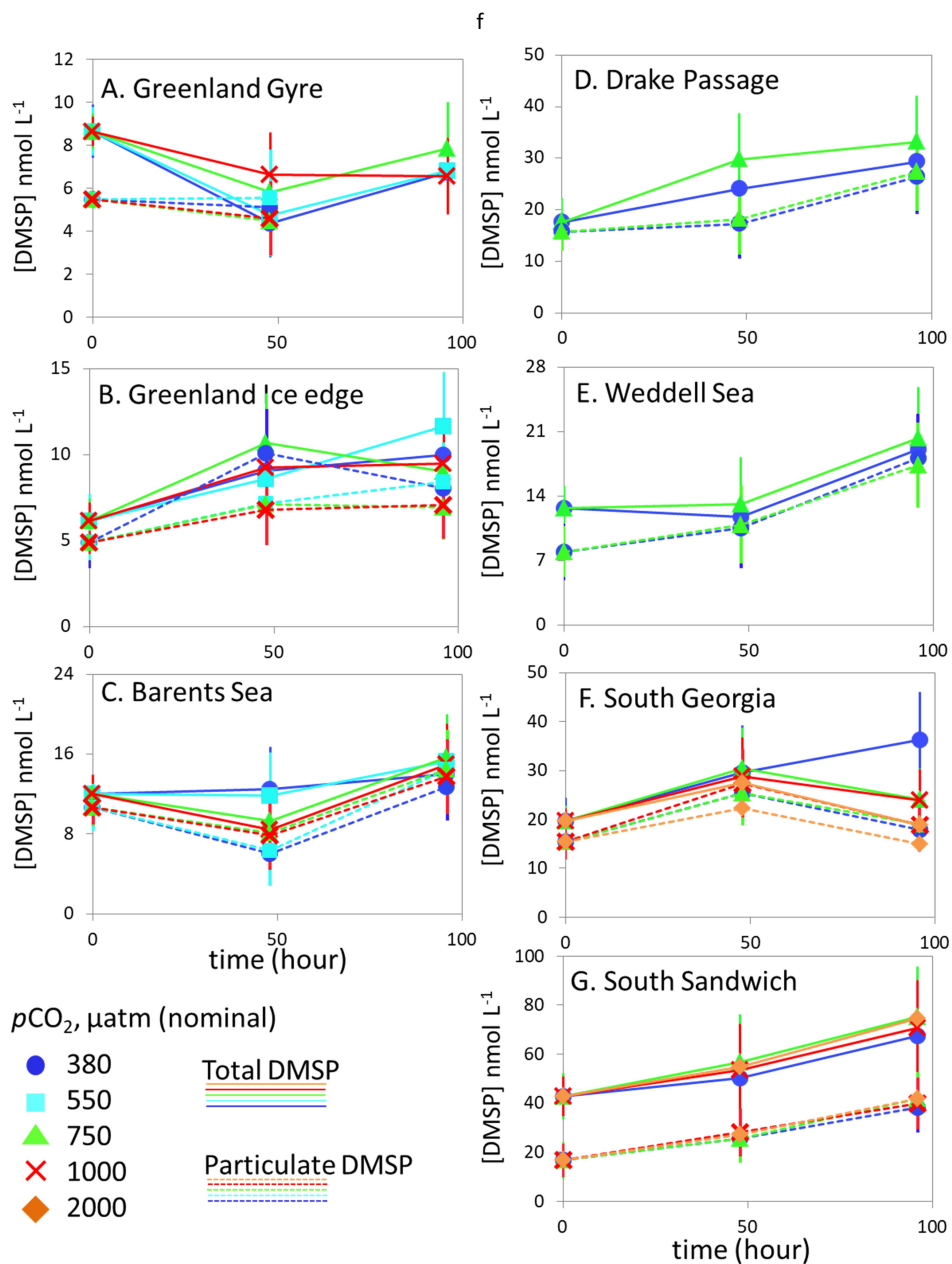
886

887 Figure 4. Total DMSP (solid lines) and particulate DMSP (dashed lines) concentrations (
888 nmol L^{-1}) during experimental microcosms performed in Arctic waters (A - C) and in
889 Southern Ocean waters (D – G). Error bars show standard error. Locations of water collection
890 for microcosms shown in Figure 1 C – F. Particulate DMSP concentrations were used in
891 calculations of DMSP production rates (Figure 5).

892
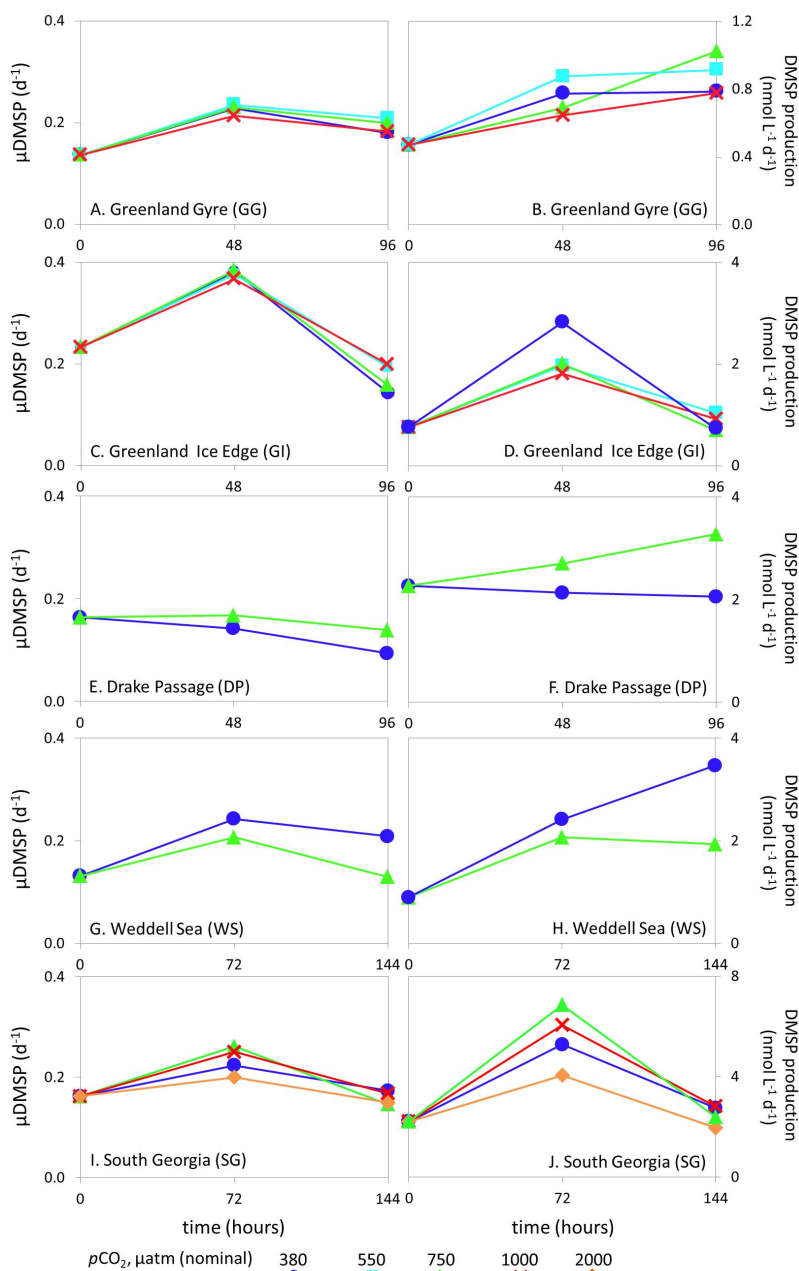
Figure 5. De novo synthesis of DMSP (μDMSP, d^{-1}) (left column) and DMSP production rates (nmol L^{-1} d^{-1}) (right column) for Arctic Ocean stations *Greenland Gyre* (A,B), *Greenland Ice-edge* (C, D) and Southern Ocean stations *Drake Passage* (E, F), *Weddell Sea* (G, H) and *South Georg*ia (I, J). No data is available for *Barents Sea* (Arctic Ocean) or *South Sandwich* (Southern Ocean).

898
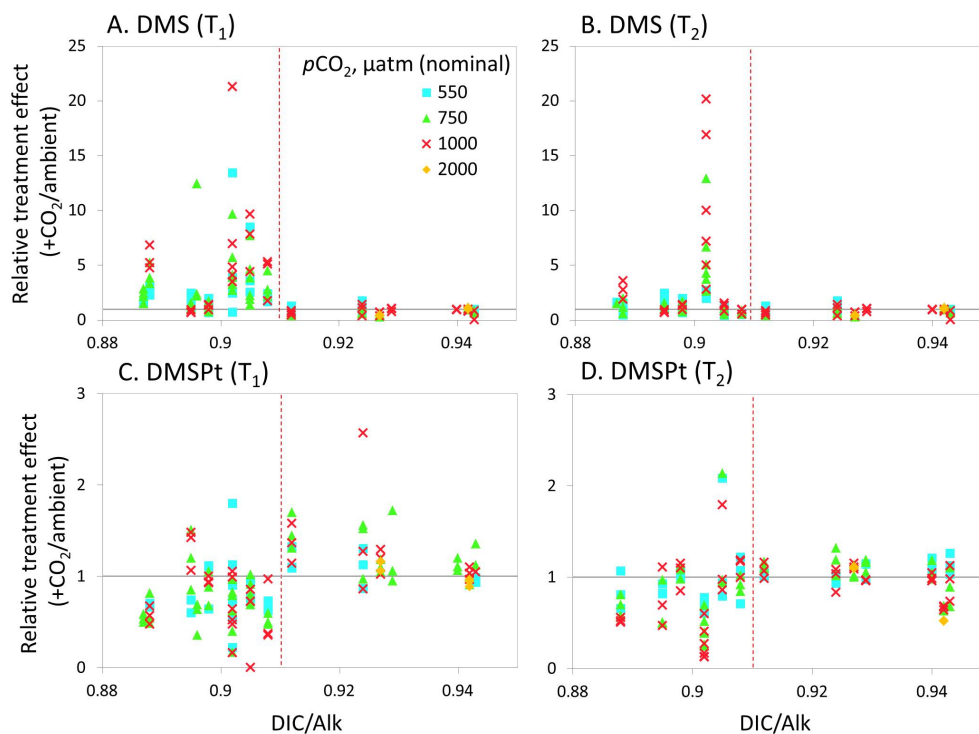
899

900   Figure 6. Relationship between the ratio of DIC to total alkalinity (DIC/Alk) of the sampled
901   water and the relative CO_2 treatment effect at ($[x]_{highCO2}/[x]_{ambientCO2}$) for concentrations of
902   DMS at T_1 (A) and T_2 (B), and for total DMSP concentrations at T_1 (C) and T_2 (D) for all
903   microcosm experiments performed in NW European waters, sub-Arctic and Arctic waters,
904   and the Southern Ocean. Grey solid line (= 1) indicates no effect of elevated CO_2. DIC/Alk
905   >0.91 = polar waters (indicated by red dashed line). T_1 = 48 h, except for WS and SG (72 h)
906   and SS (96 h). For detailed analyses of the NW European shelf data, see Hopkins & Archer
907   (2014).
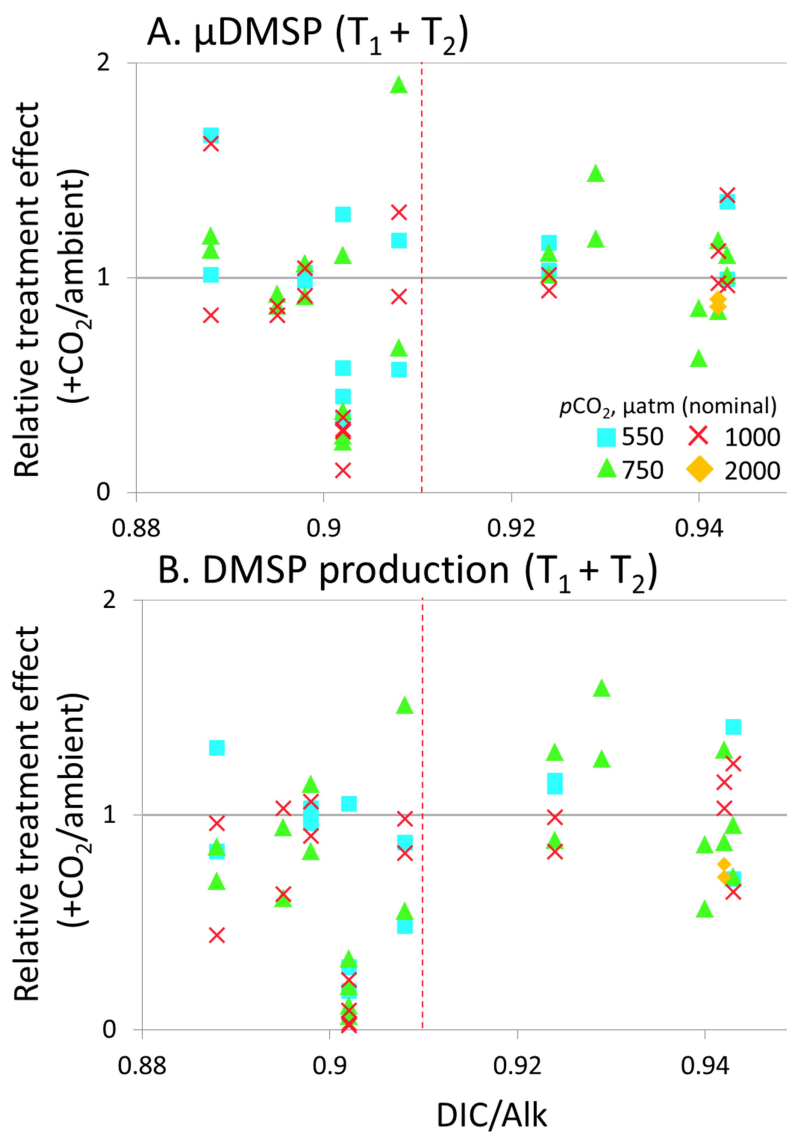
Figure 7. Relationship between the ratio of DIC to alkalinity (DIC/Alk) of the sampled water
and the relative CO_2 treatment effect at ($[x]_{highCO2}/[x]_{ambientCO2}$) for de novo DMSP synthesis
(μDMSp, d^{-1}) at T_1 (A) and T_2 (B), and DMSP production rate (nmol L^{-1} d^{-1}) at T_1 (C) and T_2
(D) for microcosm experiments performed in NW European waters, sub-Arctic and Arctic
waters, and the Southern Ocean. Grey solid line (= 1) indicates no effect of elevated CO_2.
DIC/Alk >0.91 = polar waters (indicated by red dashed line). T_1 = 48 h, except for WS and
SG (72 h). For discussion of the NW European shelf data, see Hopkins & Archer (2014).

916
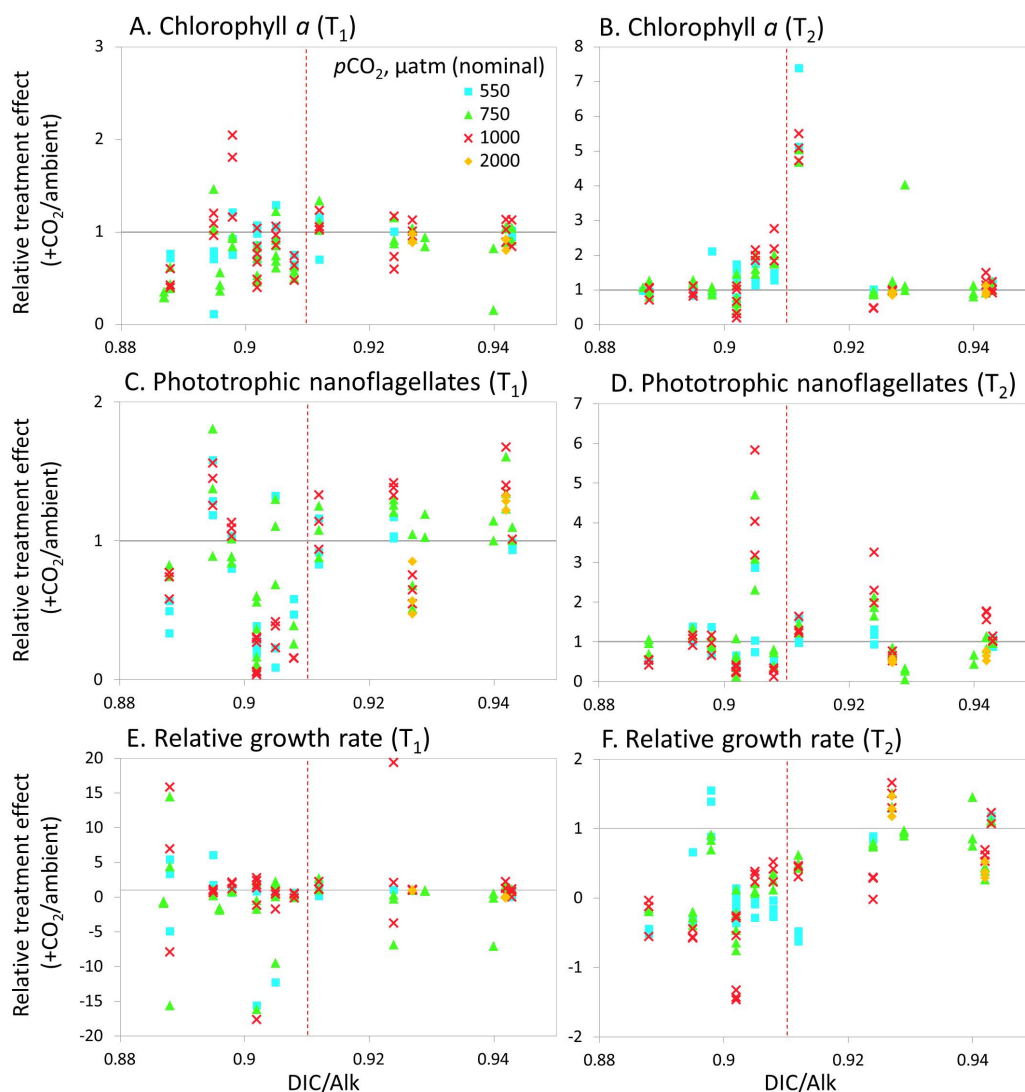
Figure 8. Relationship between the ratio of DIC to total alkalinity (DIC/Alk) of the sampled
water and the relative CO_2 treatment effect ($[x]_{highCO2}/[x]_{ambientCO2}$) for chlorophyll a
concentrations at T_1 (A) and T_2 (B), phototrophic nanoflagellate abundance at T1 (C) and T2
(D), and relative growth rate at T1 (E) and T2 (F) for all microcosm experiments performed in
NW European waters, sub-Arctic and Arctic waters, and the Southern Ocean. Grey solid line
(= 1) indicates no effect of elevated CO_2. DIC/Alk >0.91 = polar waters (indicated by red
dashed line). T_1 = 48 h, except for WS and SG (72 h) and SS (96 h).
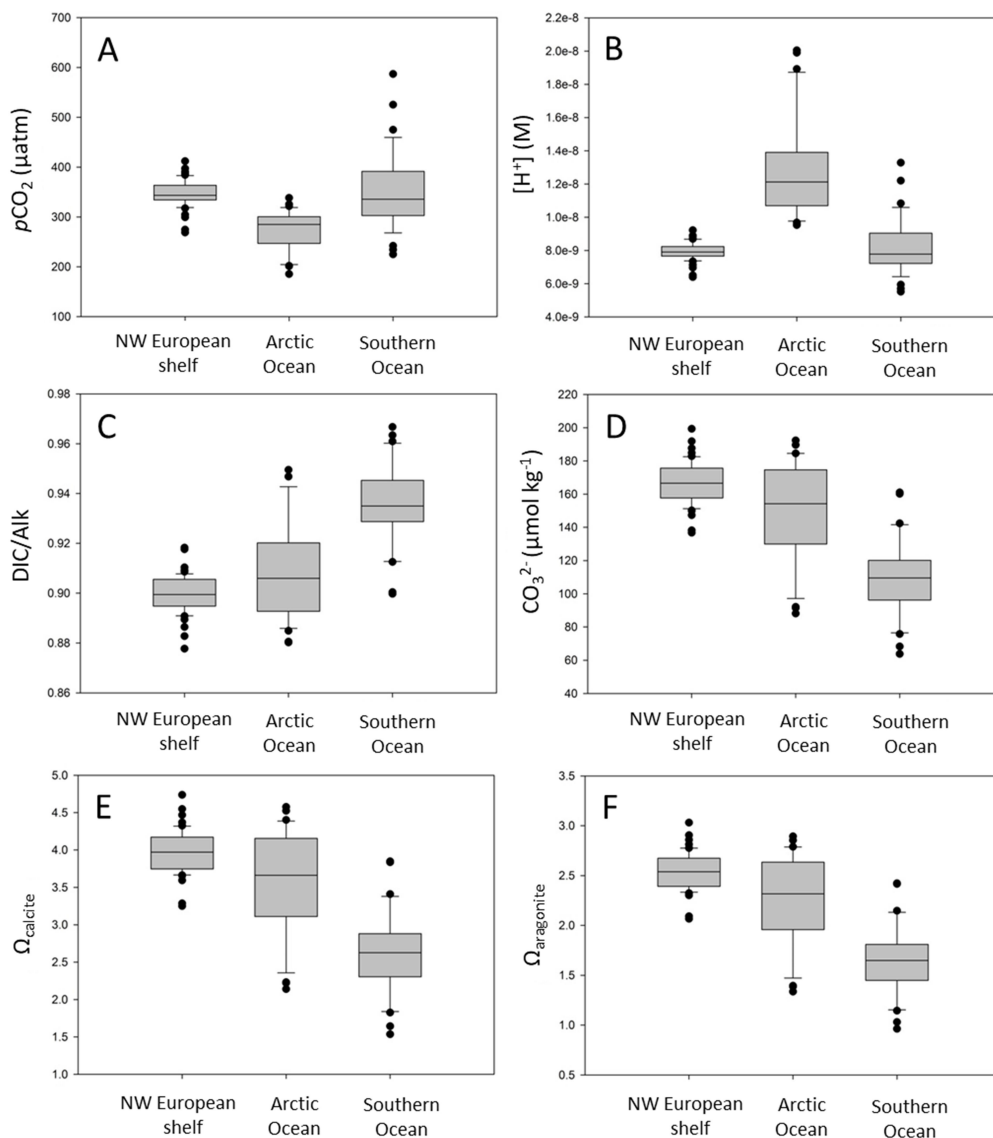
924

925   Figure 9. Variation in underway surface ocean carbonate chemistry parameters across the

926   NW European shelf, Arctic Ocean and Southern Ocean for each of the cruises in this study.

927   A. Seawater pCO$_2$ (µatm), B. Seawater [H$^+$] (M), C. DIC to total alkalinity ratio (DIC/Alk),

928   D. Carbonate ion concentration (CO$_3$$^{2-}$) (µmol kg^{-1}), E. Calcite saturation state ($\Omega_{calcite}$), F.

929   Aragonite saturation state ($\Omega_{aragonite}$).

930